MASTER'S THESIS

Development of Vision Payload for the Nanosatellite VELOX-I

Vineel Kumar Kadarla

Master of Science (120 credits)
Space Engineering - Space Master

Luleå University of Technology
Department of Computer Science, Electrical and Space Engineering

LULEÅ UNIVERSITY OF TECHNOLOGY

Development of Vision Payload for the Nanosatellite VELOX-I

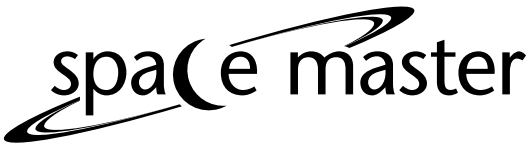

Vineel Kumar Kadarla

Supervisor

Assoc Prof Dr. Low Kay Soon
Satellite Research Center
ESKLow@ntu.edu.sg

Examiners

Dr. Anita Enmark
Division of Space Technology
Anita.Enmark@ltu.se

Prof. Dr. Christophe Peymirat
Université Paul Sabatier
Christophe.Peymirat@irap.omp.eu

A thesis submitted in partial fulfillment for the Master of Science in

Space Science & Technology

Department of Computer Science, Electrical and Space Engineering
LuleåUniversity of Technology

November 2012

Declaration of Authorship

I, Vineel Kumar Kadarla, declare that this thesis titled, 'Development of Vision Payload for Nano Satellite VELOX-I' and the work presented in it are my own. I confirm that:

- This work was done wholly or mainly while in candidature for a research degree at this University.
- Where I have consulted the published work of others, this is always clearly attributed.
- Where I have quoted from the work of others, the source is always given. With the exception of such quotations, this thesis is entirely my own work.

Signed: _____

Date: _____

"People don't choose their careers; they are engulfed by them."

John Dos Passos

LULEÅUNIVERSITY

Abstract

Division of Space Technology
Department of Computer Science, Electrical and Space Engineering

Master of Science

by Vineel Kumar Kadarla

In the recent years, CubeSat's are evolving from purely educational tools to a standard platform for technology demonstration and miniaturized scientific instrumentation. The use of COTS (Commercial-Off-The-Shelf) components aided the ongoing miniaturization of several technologies and demonstrated successfully. Furthermore advantages in this small satellite approach are due to their lesser development times and smaller sizes suitable for multiple CubeSat launches on a single launcher into their respective designated orbits which is cost effective for Universities. These architectures not only promise the combination of both temporal resolution of GEO missions with spatial resolution of LEO missions, but also breaks the trade off in conventional Earth observation satellite designs. A thorough implementation of the firmware of vision payload of the Nano Satellite VELOX-I for the Earth observation and remote sensing purposes, in the near future with high scientific payoff is presented here. In course of implementation various case studies have been learned, current date CCSDS recommendations for image compression have been considered. Effect of key components such as power, memory and data transmission capability for small satellite remote sensing applications are discussed. Implementation of the core firmware of the payload and serial interface development in Java on Linux platform of Payload Processing Unit shall be able to inherit into the future VELOX missions.

Acknowledgements

This thesis was conducted within VELOX program at Satellite Research Center, at Nanyang Technological University. I would like to express my deep-felt gratitude to my supervisor, Assoc Prof. Low Kay Soon (Director, Satellite Research Center) for providing me an opportunity. And would like to express my sincere thanks to Dr. Chen Shoushun and his team for their support in providing me the necessary background information for the project. Jan P Hakenberg guidance and review in implementation of project is exemplary. I would like to thank Project Managers Richard Bui and Lim Lip San, academic coordinators Ms.Janet, Ms.Pamela and all other colleagues of Satellite Research Center for their extensive support.

I am very grateful to my examiner, Dr. Anita Enmark for her supervision and acceptance of the topic for thesis work. I am deeply indebted to Space Master coordinator Dr. Victoria Barabash, for her constant support in every instinct of my space master years. I would extend my thanks to Dr. Johnny Ejemalm, Space Master thesis coordinator at LTU and Prof. Christophe Peymirat at UPS for helping me out in the registration of my thesis topic at respective Universities. I would like to extend my gratitude to Anette Snällfot Brändström and Maria Winnebäck for their support in administrative issues along my stay in Kiruna.

I would also like to thank all my friends, sister, cousin, my mom and dad for their unconditional love, support in every new adventure i decide to start, and this thesis is dedicated to all of them.

I want to give a special acknowledgement to the European Commission for Culture & Exchange and the Space Masters consortium for the Erasmus Mundus scholarship that allowed me to pursue studies.

Vineel Kumar Kadarla

Contents

List of Figures

List of Tables

Abbreviations

CMOS	**C**omplementary **M**etal **O**xide **S**emiconductor
DWT	**D**iscrete **W**avelet **T**ransform
DPCM	**D**ifferential **P**ulse **C**ode **M**odulation
FPGA	**F**ield **P**rogrammable **G**ate **A**rray
JPEG	**J**oint **P**hotographic **E**xperts **G**roup
OBDH	**O**nboard **B**oard **H**andling **U**nit
SBC	**S**ingle **B**oard **C**omputer
SaRC	**Sa**tellite **R**esearch **C**enter
SNR	**S**ignal to **N**oise **R**atio
PPU	**P**luggable **P**rocessor **U**nit
OBC	**O**n **B**oard **C**omputer
LEO	**L**ow **E**arth **O**rbit
GSD	**G**round **S**ample **D**istance
COTS	**C**ommercially **O**ff **T**he **S**helf
CCSDS	**C**onsultative **C**ommittee for **S**pace **D**ata **S**tandards

Dedicated to loving mom & dad

Chapter 1

Introduction

Nano Satellite class of satellites is a proven cost effective approach for Earth observation missions with limitations of spatial resolution. 3U CubeSat which falls under this class allow user to develop the various applications under the common bus architecture based on COTS components. Generally, imaging systems are developed as an individual sub system apart from the bus architecture owing to essential constraints like mass, power, size, etc., in case of special segment of the Nano Satellite class, 3U CubeSat. The main purpose of development of the vision payload is to capture the Earth images at an altitude 650 - 700 km, Sun synchronous low earth orbit (LEO) for remote sensing application. Vision payload is developed as an individual subsystem, and shall be integrated on to the Nano Satellite VELOX-I. Earth remote sensing helps in studying various phenomena related to Earth surface. The range of applications varies from agriculture, geology, coast and marine studies to urban development and environmental affairs. Remote sensing satellites are equipped with payload sensors that capture images and aggregate data of Earth surface. The gathered information is then transmitted for further processing and analysis. Satellite mission is one of the main factors that determines satellite overall dimensions, weight, and cost.[5] On the other hand, this limits the final specifications to those of the components available in market. For instance, the final Ground Sample Distance (GSD) is limited by the available commercial camera systems, which usually do not meet dimensions and resolution requirements simultaneously. A better GSD can be achieved if a customized optical design is adopted besides choosing off the shelf.

The payload comprises of three main modules:

- CMOS Sensor
- FPGA data acquisition board.
- Payload Processing Unit

In order to achieve the necessary (primary) objective of the payload i.e., to capture the Earth images from such an altitude and the harsh environment, makes the payload to consider the following absolute requirements.

- Radiation Environment:
  ✓To overcome the difficulty, a radiation tolerant CMOS sensor have been designed and developed in house at Satellite Research Center, NTU.

- Optical Lens:
  ✓In order to satisfy the requirements of altitude and the ground sampling distance of ~ 70 meter, need for the design of optics is inevitable and manufacturing process is outsourced.

1.1 Problem Statement

Most CubeSat employ a high resolution camera on-board and it is inevitable that the images captured by the camera are larger than what can be sent to the ground station in a single pass over the ground station. The purpose of Nano Satellite (VELOX-I) is to capture images of the Earth and relay these images to the ground station with the limited resources at hand. The focus of this research is to develop the firmware for the full functionality of the vision payload and implement necessary compression algorithms, and a detailed study on how these tasks are achieved without affecting the image quality as well as a suitable design and firmware implementation is presented.

1.2 Research Objectives

The objective of this thesis is to develop the firmware for the vision payload for an Earth observation Nano Satellite VELOX-I. In order to achieve the main objective, a number of sub-objectives are identified and executed.

- Image Acquisition:
  ✓Interfacing to the CMOS sensor to the Payload Processor Unit(PPU).
  ✓Controls of CMOS sensor parameters (exposure time, sensitivity, etc.,).

- Image Processing techniques:
  ✓Compress images for better storage and transfer capability.
  ✓Effective compression of the raw files.
  ✓Creation of thumbnail of images captured.

- Serial Interface development:
  ✓Development of serial interface of the payload.
  ✓Development of Image/File handling protocol for tasks like trigger, file transfer, deletion, etc.,

1.3 Structure of the Thesis

There are seven chapters presented in this thesis and their content are elucidated here as follows.
Chapter 1 provides the introduction of the project, throws light on the problem statement, motivation behind the research work and justification of its relevance by means.
Chapter 2 contains the background information of the Nano Satellite mission, payload architecture, tools used and software design methodology adopted during firmware development.
Chapter 3 explains the literature survey on issues that are relevant to development of the payload. The survey starts with a discussion on digital representation of an image, factors effecting the image acquisition, theory behind image compression and various techniques available are presented. And first part of the thesis to investigate into viable compression techniques based on the computational complexity and payload hardware are studied, compression algorithms were implemented in MATLAB model and results are presented.
Chapter 4 contains the second part of the thesis' main contribution. This chapter starts with the discussion of some key aspects of the payload development such as configuration of the CMOS Sensor via FPGA, various control parameters and artifacts of the sensor design and overcoming of those by means of different calibration techniques are presented. File handling structure, various storage formats and exporting of these are explained with details.
Chapter 5 describes the payload interface development, introduction to the serial UART interface and various parameters involved in configuring the serial port for the payload are illustrated with necessary example codes.

Chapter 6 presents payload handling protocol developed with the help of the control flow diagram, various functionality of payload are described under respective sections. Chapter 7 concludes with the research outcome of the thesis, and suggests some possible research work that can be done in the future to extend the outcome of present research.

1.4 Work Methodology

In order to achieve the expected results in prescribed definitive time line, the work plan is divided into three phases, and is also represented by Figure [1.1]

1. Literature Review
   In this phase, numerous similar implementations and their strategies in course of development are studied and primary modules were implemented in MATLAB.

2. Design Phase
   In this phase, a detailed software architecture which is backbone for the payload firmware development is proposed.

3. Implementation, Integration & Test Phase
   In this phase, the proposed software architecture in the earlier phase is implemented module by module, after implementation of the complete desired functionality software codes are integrated and progressively tested in order to avoid system malfunctioning.

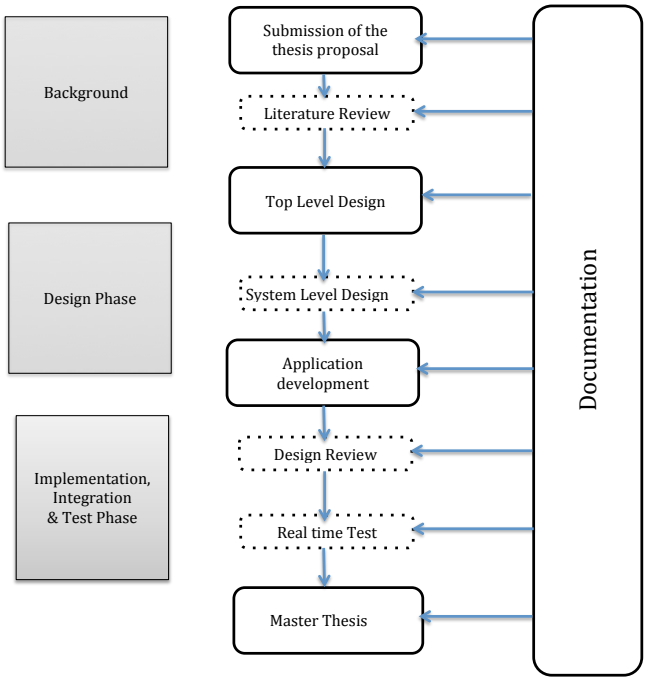

FIGURE 1.1: Work Methodology

Chapter 2

Background

A new class of Pico satellite, the CubeSat project began as a collaborative effort between Prof. Jordi Puig Suari at California Polytechnic State University (Cal Poly), San Luis Obispo, and Prof. Bob Twiggs at Stanford university in 1999. The main purpose of the project is to provide a standard for design of pico satellites to reduce cost and development time, increase accessibility to space, and sustain frequent launches. A standard one unit (1U) CubeSat occupies volume of 10x10x10 cm^3 and weights no more than 1.3 kg. CubeSat, made from off the shelf components, provide a low cost platform and development time that is relatively small compared to conventional larger size satellites.[6] Primary responsibility of the developers is to ensure the safety and success of CubeSat missions hence they developed guidelines and the one who wants to develop the CubeSat must follow these guidelines. For all the above reasons companies, governmental organizations, and universities expressed a growing interest in CubeSat as a low cost mean of doing scientific space research missions and for testing and space qualification of next generation of small payloads in space. Moreover, a CubeSat provides very useful educating tools that train students and space engineers using real world satellite experience. 3U CubeSat is similar to 1U cube but has the dimensions of 30x10x10 cm^3 and weight not exceeding more than 4.5 kg.[5]

2.1 Nano Satellite Mission VELOX-I

VELOX-I is the first Singapore Nano Satellite to operate in LEO and is completely built by students of Nanyang Technological University. Students participate in the projects with the support from research students and staff. VELOX-I is planned to be launched into the Low Earth Orbit in the second quarter of 2013. Attitude determination and control system, power supply, and vision payload are developed in-house. The on-board

data handling and communication boards are commercially off-the-shelf hardware. The scientific quantum payload will be developed by the Center for Quantum Technologies. Ground Station for VHF/UHF bands has been built by NTU undergraduate students and is operational since May 2010. [7]

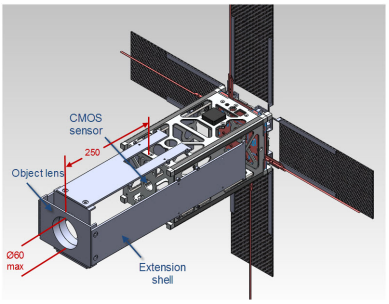

FIGURE 2.1: Artistic impression of the Nano Satellite VELOX - I

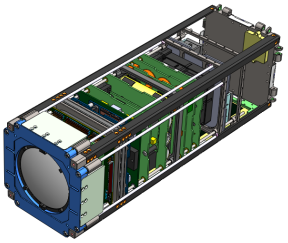

FIGURE 2.2: Structure with Vision Payload

2.1.1 Mission Objectives

- To launch the first Singapore's Nano Satellite VELOX-I. The satellite will be designed, built, and operated by students from different schools in College of Engineering, NTU.
- To place and operate the satellite in a sun-synchronous LEO.
- To acquire images of Earth and transmit them back to ground station.
  A narrow angle camera with tele-optics is used to provide high-resolution images of Earth from LEO.
- To carry out experiments relevant to technology demonstration.
  Payloads being studied: a vision system, a dual-FOV sun sensor and a quantum physics payload.

2.1.2 Technical Facts

TABLE 2.1: Facts: Nano Satellite VELOX -I

Dimensions	100 x 100 x 240 mm (N-Sat)
Mass	3500 g (N-Sat)
Expected lifetime	24 months
Orbit	Sun-synchronous LEO, altitude 650 - 700 km
ADCS **OBDH Unit**	N-Sat: 3-axis stabilized and controlled: 1 GPS receiver, 2 sun sensors, 2 IMUs, 3 magnetic torquers, 3 reaction wheels; 1 OBC with Silicon Lab's C8051F120 MCU running data handling software on Salvo ROTS; 2GB SD card for data storage; UART and I2C data interfaces
Communications	Low gain antennas for Omni directional coverage 1 dipole for UHF, 1 dipole for VHF; UHF/VHF transceiver with AFSK modulation; 9600 bps down-link / 1200 bps up-link, 1200 bps experimental inter-satellite link
Power subsystem	N-Sat: 4 deployable and 4 body-mounted 3J GaAs panels for 19.2 W BOL power; 6.0 - 8.4 V unregulated, latch-protected 5 V and 3.3 V bus; 3600 mAh Li-ion batteries
Structure	Hard anodized Al. 7075 chassis with stainless steel load bearing parts;
Thermal control	Passive: Multi-Layer Insulation (MLI) and radiators (N-Sat) N-Sat: Vision system with extended optics for ground sampling distance of 20 m
Ground segment	Ground station: NTU campus UHF/VHF high gain cross-yagi antennas for TT&C and down-link

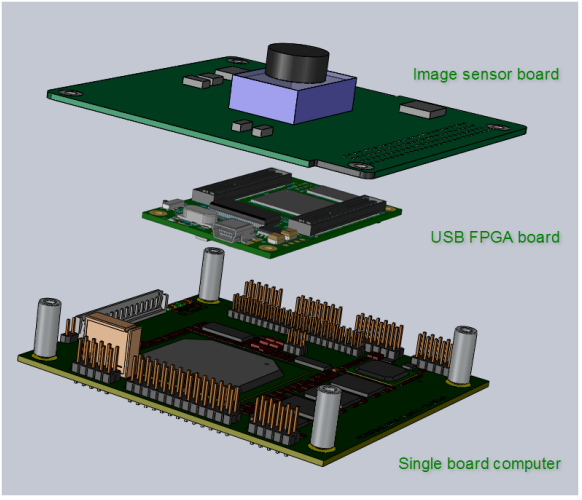

FIGURE 2.3: Conceptual Payload Architecture

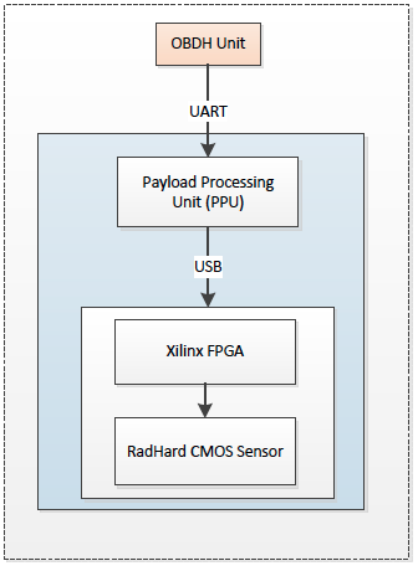

FIGURE 2.4: Block Diagram of the Payload with interfaces

2.2 Payload Architecture

The arrangement of the three modules of the Payload are as shown in the virtual image Figure 2.3 and its block diagram in the Figure {fig:block. The interface between these modules can be seen in the Figure 2.4. Payload can be communicated with other devices with Serial interface (UART) developed and CMOS image sensor configuration can be loaded and accessed by the Xilinx FPGA module with USB interface.

2.2.1 Opal Kelly XEM3005

The Opal Kelly XEM3005-1200M32P is a compact 1,200,000-gate Xilinx Spartan-3E FPGA board with 32MB RAM and USB 2.0 interface enabling an almost instant re-programming of the FPGA makes us to choose this module for data acquisition from the CMOS image sensor. It's chosen for our project for being low cost. It is designed without the power supply and that makes it better suits the end user design which is required in our case. This device makes the Software / Hardware co-processing in our case realizable.[8]

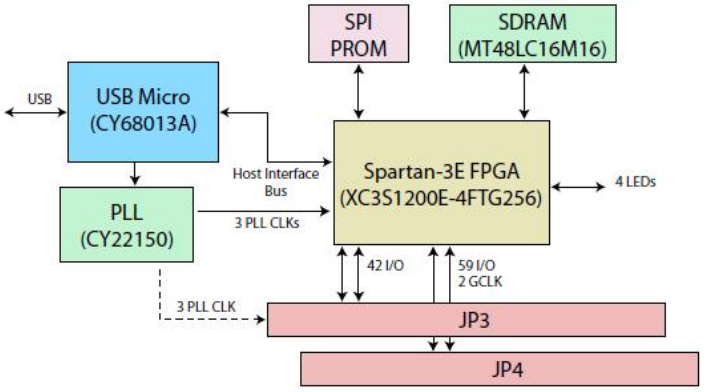

FIGURE 2.5: Opal Kelly XEM3005 architecture

2.2.2 Radiation Hardened CMOS image sensor

The Radiation tolerant image sensor chip layout for space application is as shown in the Fig **??**. The major design concerns lie within the design of the photo diode and the floating diffusion node against radiation-induced dark current. In order to adapt the sensor to the dramatic temperature change in space environment, a programmable column biasing current circuit was considered in 4T pixel architecture of the sensor design [9]

2.2.3 Pluggable Processor Module (PPM)

The Cool SpaceRunner-LX800 is a fully self-contained, rugged single board computer. Its X86-compatible AMD Geode LX800 processor comes with graphics, 256MB RAM and 2 GB solid state disk without any moving parts is as shown in the Fig 2.7. Either VGA or LVDS displays are directly supported. All standard peripherals are already integrated on board. There is a LAN interface, four USB host ports, and two serial interfaces, user configurable to handle either RS232 or RS485 levels.The Cool SpaceRunner-LX800

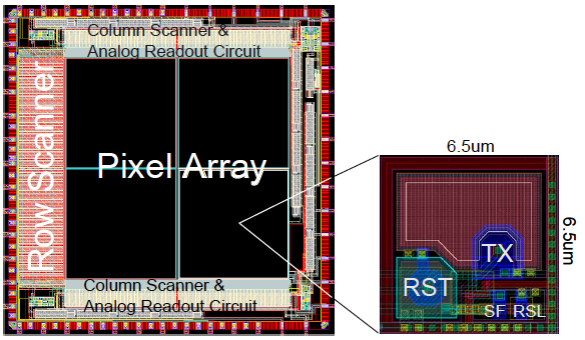

FIGURE 2.6: Radiation Tolerant CMOS image sensor

features status indication LED's and a programmable watchdog. The computer can be expanded with standard peripheral cards for the PC/104-Plus bus. This Single board fan less computer is connected to the CMOS sensor interface board with PC/014-plus. one of the USB port is connected to the XEM3005 FPGA module for CMOS sensor data acquisition and operation.[10]

Power consumption is a mere 5 watts and doesn't require cooling. The board is specified for the extended ambient temperature range of [-40 ° C, +85 ° C]. The Cool SpaceRunner-LX800 uses the LiPPERT Enhanced Management Technology (LEMT). It handles the boards housekeeping tasks like power sequencing and watchdog, and provides useful utility functions for the application. Among them is a secure, write and clear protected Flash area that can be used for security keys. LEMT also enables remote condition monitoring. With its all the above features, the Cool SpaceRunner-LX800 is the best choice for our purpose that need to operate in adverse environments. [10]

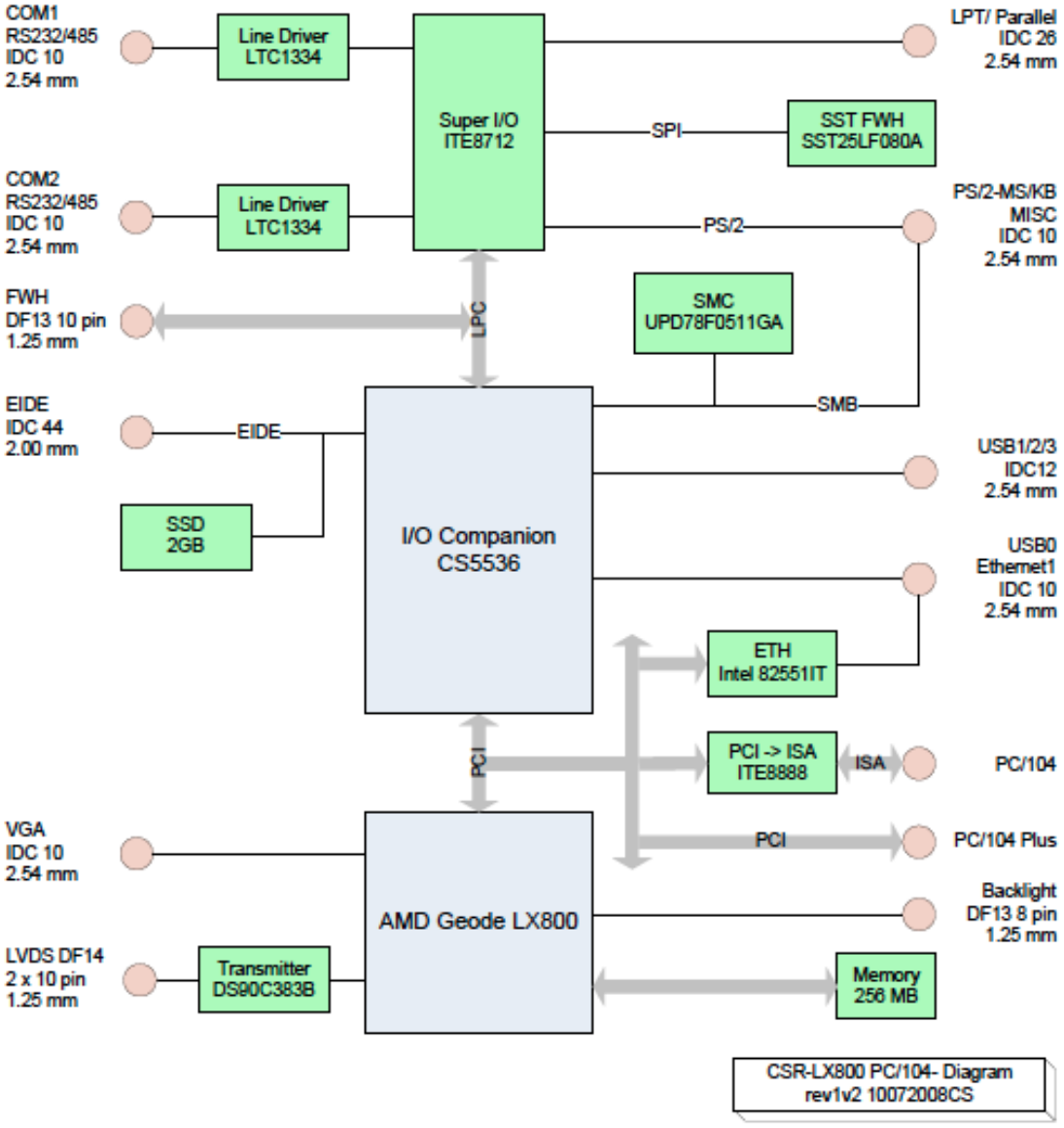

FIGURE 2.7: Internal Block diagram of SBC

TABLE 2.2: Characteristics of the Optical lens

Focal length	3.5mm - 10.5mm
Maximum Aperture Ratio	1:1.0
Maximum Image Format	4.8mm x 3.6mm (diameter 6 mm)
Operation Range Iris	F1.0 - F16C
Flange Back Length	12.5mm
Focus	0.3m - Inf
Zoom	3.5mm - 10.5mm
Object dimension at minimum object distance	3.5mm 52cm x 34.1cm 10.5mm 14.5cm x 10.8cm

2.3 Optical System

For Ground test purposes, we have chosen Computar T3Z3510CS-IR which has the characteristics that are tabled in 2.2.

FIGURE 2.8: Test optics of the Payload

The lens system operates in both visible and IR regions of the light. The lens weights 63 grams. The diameter is 41.6mm, the height is 48.8mm. The lens is attached to the PCB via CS-mount, and operates in temperatures between $-20\,^{\circ}$C to $50\,^{\circ}$C.

2.4 Operating System - Linux

Linux is a free and open source computer operating systems distributed under open source software license *GNU General Public License*. Linux was developed by Linus Torvalds initially targeting Intel x86 based computer architectures, later ported to more platforms than any other operating system. Linux due to its portability became predominant in embedded system developers. Linux kernel can be ported to both memory and memory less embedded system devices. Many Linux distributions were available til date, for our project purpose we have considered more popular and yet lite Debian kernel for payload application development.

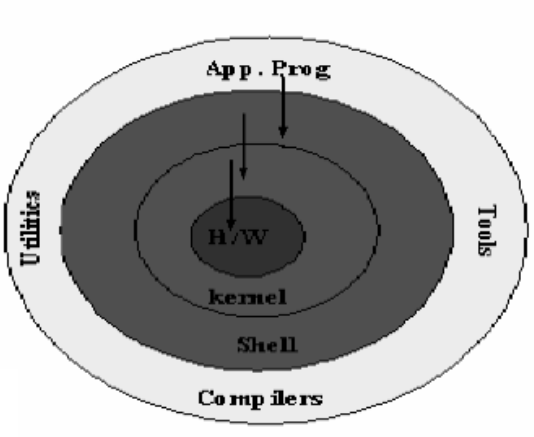

FIGURE 2.9: Linux Internal Architecture

2.4.1 Internal Architecture

The Linux operating system has unique architecture consists of kernel and shell as its major components.

1. Shell: It is part of the operating system (OS), which serves as an intermediate between the user and the OS.
2. Kernel: This serves as a direct interface between the hardware and the OS. Performs operations such as creation, deletion of the processes, scheduling of the process management. Provides the mechanisms for synchronization of the processes and inter process communication.

2.4.2 System Architecture

The decomposition of the Linux Operating System can be as shown in the Figure 2.10 In Linux, everything is considered as a file other than the processes itself.

- User Applications: The user applications are developed in this layer.
- Operating System Services: These services are the part of the OS which also provide interface to the Kernel.

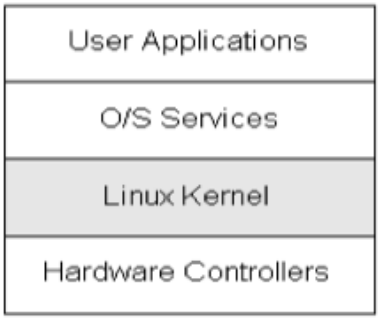

FIGURE 2.10: Linux System Architecture

- Linux Kernel: The Linux Kernel abstracts and mediates access to the hardware resources including the processor.
- Hardware Controllers: This sub-system consists of all the physical devices in the Linux installation, devices such as Memory, Processor, USB drives and network infrastructure.

2.5 Programming Languages & Environment

Application framework of the Payload is developed in Java, while the serial interface developed in C/C++. In Course of sensor calibration, GUI has been developed in Java. MATLAB is used for the validation of the Image Processing (compression) algorithms as a proof of concept before implementation in the real time framework and also to read raw image. Open source integrated development environment Eclipse is chosen for firmware development on Linux due to its huge support from the developer's community and cross-platform compatibility.

2.6 Software Design Methodology

In order to achieve success in success in large software packages, some kind of strategy or design methodology is mandatory. Essential steps of software development regardless of size and complexity of the project are analysis and coding and is as shown in Figure 2.11. More Complex projects needed sophisticated approach with sections such as requirements capture in the preceding stage of analysis and followed by program design and testing in the manner shown in 2.12. From the lessons learned, the implementation of the methodology in Figure 2.12 may invite unnecessary risks an failure. Hence, an iterative interaction between the development phases is appreciable and followed in this project.

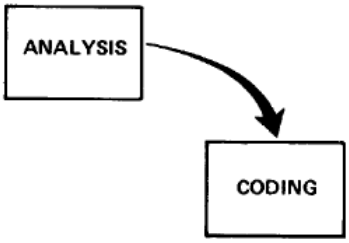

FIGURE 2.11: Implementation steps for small software packages

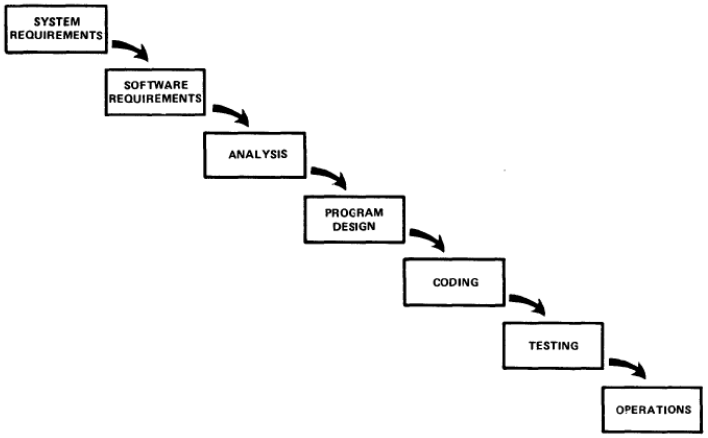

FIGURE 2.12: Implementation steps for large software packages

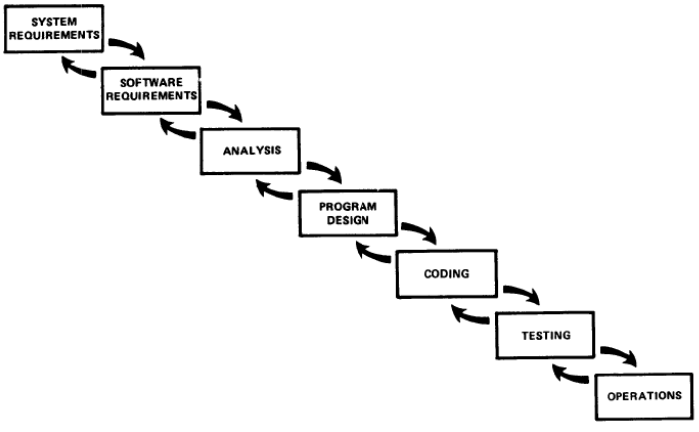

FIGURE 2.13: Iterative interaction between software design stages

Chapter 3

Literature Review

3.1 Digital representation of the images

An image may be defined as a two-dimensional function, $f(x,y)$, where x and y are spatial (plane) coordinates, and the amplitude of f at any pair of coordinates (x,y) is called *intensity* or *grey scale* of the image at that point. When x,y and the intensity values of f are all finite, discrete quantities, we call the image as *digital image.*[11]
A digital image $f[m,n]$ described in a two-dimensional discrete space is derived from an analog image $f(x,y)$ in a continuous space through a *sampling* process that is termed as *digitization.* A two-dimensional continuous image $f(x,y)$ as shown in Fig 3.1 is divided into *N rows* and *M columns.* And the intersection of the row and the column is termed as *pixel.* In most cases, which we might consider to be the physical signal that impinges on the face of a two-dimensional sensor, is actually a function of many variables including depth (z), color (λ) and time (t). The value assigned to every pixel is the average brightness in the pixel rounded to the nearest integer value. The process of representing the amplitude of the two-dimensional signal at a given coordinate as an integer value with L different gray levels is usually referred to as *quantization* [1].

3.1.1 Integrated CMOS image Sensor

Image sensors are manufactured in wafer foundries or fabs, these tiny circuits and devices are etched onto silicon chips. The biggest problem with CCD is that there isn't enough economy of scale. They are created in foundries using specialized and expensive processes that can only be used to make CCD. Today CMOS is the most common method for manufacturing processors, image sensors and memories due to their high volume process and low cost feature. There are two basic kind of CMOS image sensors available today.

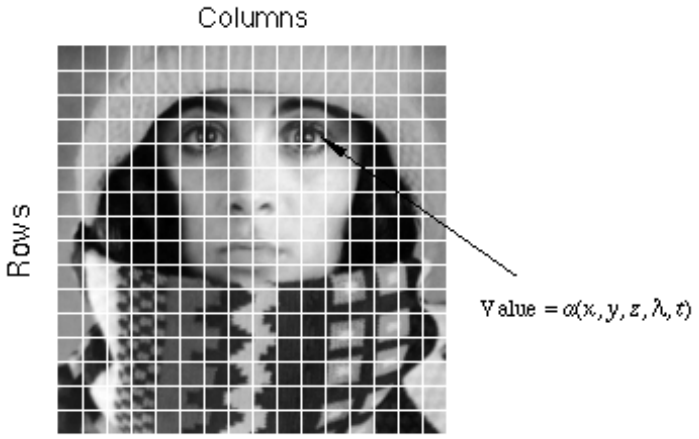

FIGURE 3.1: Digital representation of an image [1]

While these image sensors are inexpensive, they suffer from the Fixed Point Noise (FPN) that resulted from each picture element having its own amplifier. Due to the unmatched offset and gain characteristics between each amplifiers, they shall impose same noise pattern on every image.

- **Passive Pixel Sensors** (PPS) were the first image-sensor devices used in the 1960s. In passive-pixel CMOS sensors, a photo site converts photons into an electrical charge. This charge is then carried off the sensor and amplified. These sensors are small and just large enough for the photo sites and their connections. The problem with these sensors is noise that appears as a background pattern in the image. To cancel out this noise, sensors often use additional processing steps.
- **Active Pixel Sensor** (APS) reduce the noise associated with passive-pixel sensors. Circuitry at each pixel determines what its noise level is and cancels it out. It is this active circuitry that gives the active-pixel device its name. The performance of this technology is comparable to many charge-coupled devices (CCDs) and also allows for a larger image array and higher resolution.[9]

3.1.2 Imager Facts

CMOS image sensors can incorporate other circuits on the same chip, eliminating the many separate chips required for a CCD. This also allows additional on-chip features to be added at little extra cost. These features include anti-jitters (image stabilization) and image compression. Not only does this make the camera smaller, lighter, and cheaper; it also requires less power so batteries last longer. It is technically feasible but not economic to use the CCD manufacturing process to integrate other camera functions,

such as the clock drivers, timing logic, and signal processing on the same chip as the photo sites. These are normally put on separate chips so CCD cameras contain several chips, often as many as 8, and not fewer than 3.CMOS image sensors can switch modes on the fly between still photography and video. While CMOS sensors excel in the capture of outdoor pictures on sunny days, they suffer in low light conditions. Their sensitivity to light is decreased because part of each photo site is covered with circuitry that filters out noise and performs other functions. The percentage of a pixel devoted to collecting light is called the pixel's fill factor. CCD's have a 100% fill factor but CMOS cameras have much less. The lower the fill factor, the less sensitive the sensor is and the longer exposure times must be. Too low a fill factor makes indoor photography without a flash virtually impossible. To compensate for lower fill-factors, micro-lenses can be added to each pixel to gather light from the insensitive portions of the pixel and *focus* it down to the photo site. In addition, the circuitry can be reduced so it doesn't cover as large an area. The quality of an image depends on the number of bits to represent an image, more the number of bits more sharper the image. The radiation tolerant CMOS image sensor developed in house at VIRTUS IC Design Center, NTU is of 12 bit.[9] [12]

3.1.3 Fill factor

Fill factor represents to the percentage of a photo site that is sensitive to light. Higher the fill factor, higher sensitive to light and thus represents the good image sensor. In the Fig 3.2, the photo detector represents the photo site that is sensitive to light and the rest is the sensor circuitry.[9]

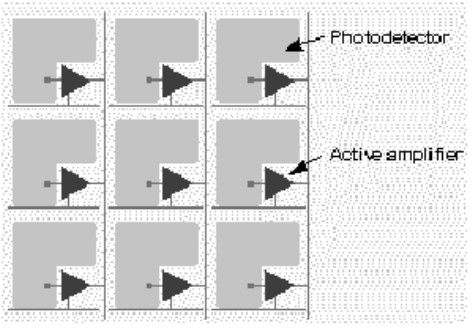

FIGURE 3.2: Fill factor of the Pixel

3.1.4 Noise

Noise may be defined as an unwanted electrical signal that interferes with the image being read and transferred by the image sensor. There are two types of noises generally associated with the CMOS image sensors.

1. Read Noise: This noise is more generic random noise which is generated by the noise characteristics of the associated electronics. This noise is also known as temporal noise.
2. Fixed Pattern Noise: is a distortion that appears in an image due to variations of device parameters across the sensor.

3.1.4.1 Fixed Pattern Noise

FPN effects the performance and quality of the image sensors, and usually refers to non-temporal spatial noise which is due to device mismatch in pixels and color filters, between the multiple gain amplifiers, ADC etc., FPN can be characterized as coherent or non-coherent.
The most usual and hard noise in image sensors is associated with detectable row-wise or column-wise artifacts which are due to mismatches in the multiple signal paths, and un-correlated, row-wise operations in the image sensor. This type of noise is coherent in nature and in general can be eliminated by reference frame subtraction.
Apart from the type of FPN discussed in earlier paragraph, most frequent FPN are dark current FPN and FPN due to gain mismatches which are more difficult to remove as the lead times to eliminate them are higher and dependent on the hardware.

3.1.5 Aspect Ratio

The ratio between the height and width of the sensor, derived from division of vertical number of pixels(height) by horizontal number of pixels (width) leaving it in the fractional format.
Here in our case, 786 x 512 CMOS sensor would give an aspect ratio of 1.535 [9]

3.2 Storage Capacity

The imaging processing hardware of 3U CubeSat shall process the raw input image from the payload through necessary steps such as filtering, compression and is stored. The

output images, according to our mission requirements is store in memory of the SBC which is in turn transferred to OBDH via serial interface and transmitted back to Earth. This storage capability is not useful if the data rates are not increased accordingly. In fact, it is trivial to show that there is a linear relationship between storage capability and data rate if the constraint is enforced to have enough storage capability to store all the images that can be downloaded in one access to the ground station:

$$Storage(MB) = 15/2\delta T(\frac{min}{access})R_b(Mbps) \tag{3.1}$$

where Storage(MB) is the storage capability required to be able to empty the memory during one access to the ground station in MB; $\delta T(\frac{min}{access})$ is the average duration of an access to the ground station in minutes, $R_b(Mbps)$ is the down-link data rate in Mbps, and the factor $\frac{15}{2} = \frac{60}{8}$ comes from transforming bits into bytes and minutes into seconds. For $R_b = 0.25$ Mbps, and δT=5($\frac{min}{access}$), a storage capability of Storage(MB)= 9.3 MB is required, which is much lower than what can be achieved in CubeSat. It follows that the real limiting factor is data rates, and not data storage. Furthermore, we note that payloads that would have high requirements in terms of data storage such as hyper-spectral image sensors are probably also incompatible with current CubeSat technology because of other limitations, namely available power and space [13].

3.3 Image Compression

In general digital images need huge amount of space for their storage and require larger bandwidths for transmission. The goal of the image compression is to reduce the amount of data needed to represent the digital image. This in turn reduces amount of disk space needed to store the image (in bytes) and improvises the disk capability to store larger amounts of data. Further more it also lowers the bandwidth requirements in transmission channels. 9/7 Wavelet filter based compression technique is chosen as it is less computationally complex and targeted at Low powered devices (aka Small Satellites). Ultimate choice was made due to the Nano Satellite mission constraints (image quality, storage memory, bandwidth and power).[11]

3.3.1 Types of redundancies

Data compression aims to reduce the amount the data required to represent a given quantity of information while preserving as much information as possible. Here, in the definition data and information are not the same; data are the means by which the information is conveyed. The same information can be represented by various amounts of

data which contain repetitive and irrelevant information are said to contain *redundant data.*

If we let a and a' denote the number of bits in two representations of the same information, the *relative data redundancy* R of the representation with a bits is

$$R = 1 - \frac{1}{C} \tag{3.2}$$

where is C, is commonly called the *compression ratio* and is defined by

$$C = \frac{a}{a'} \tag{3.3}$$

Image compression and coding techniques explore three types of redundancies : Coding redundancy, Inter-pixel (spatial/temporal) redundancy and Psycho-visual redundancy.

3.3.1.1 Coding Redundancy

A code is a system of symbols (i.e.,bytes, bits) that represents information. Each piece of information is represented by a set of code symbols. The gray level histogram of an image can be used in construction of codes to reduce the data used to represent it. Given the normalized histogram of a gray level image where

$$p_r(r_k) = \frac{n_k}{n} \tag{3.4}$$

Where k = 0,1,2,..., L - 1, r_k is the pixel values defined in the interval [0,1] and $P_{r(k)}$ is the probability of the occurrence of r_k, L is the number of gray levels, n_k is the number of times that k^{th} gray level appears and n is the total number of pixels. **??**book)
Average number of bits used to represent each pixel is given by

$$L_{avg} = \sum_{k=0}^{L-1} l(r_k) p_r(r_k) \tag{3.5}$$

3.3.1.2 Inter pixel Redundancy

The pixel values of an image are often correlated, there can be large spatial regions in which the pixel values are clustered around the given intensity or color. Because of these pixels when we try to encode the intensity of each pixel, the information is unnecessarily replicated in the representation of the neighboring pixels. The type of redundancy that take form for images is spatial redundancy and for video it is temporal(or interframe)redundancy.Mapping technique is used in removal of inter-pixel redundancy and is

a reversible process. Original image can be reconstructed from the transformed pixel values.Compression techniques such as CAC,(1-D, 2-D)Run Length Encoding techniques, DPCM has inherent behavior of removal of inter-pixel redundancy.[11]

3.3.1.3 Psycho-visual Redundancy

Most 2-D intensity arrays contain information that is ignored by the human visual system. So, compression techniques should aim in reducing the data that is psycho-visually redundant.The elimination of this data is possible because the information itself is not essential for visual processing but it leads to the omission of data with quantitative information and is commonly referred to as *quantization*. This is an irreversible process and leads to loss of image quality when reconstructed. Many compression techniques exploit this type of redundancy. For instance, JPEG uses DCT of image pixel followed by quantization of their coefficients. [11]

3.4 Measuring Image Information

The information in an image can be modeled as a probabilistic process, where we first develop a statistical model of the image generation process. The information content (entropy) can be estimated based on this model. The information per source (symbol or pixel), which is also referred as *entropy* and is calculated by:

$$H = -\sum_{j=1}^{J} P(a_j) log P(a_j) \tag{3.6}$$

Where $a_j$represent the *source symbols*, $P(a_j)$ refers to the the source symbol / pixel probability. J refers to the number of symbols or different pixel values.

3.5 Image Compression Model

An image compression system typically composed of two distinct functional components: an encoder and a decoder. Whereas the encoder performs the *compression*, and the decoder performs the complementary operation to the earlier know as *decompression*. Both operations can be performed using software/hardware or the combination of both firmware and hardware. For our mission criteria, we deploy the compression algorithms in software.
Input image *f(x,...)* is fed into the encoder, which creates the compressed representation

of the input, and when the compressed representation is presented to decoder,a reconstructed output of the input image *f' (x,..)* is generated. If the compression system used is loss less, the reconstructed image is an exact replica of the original image.

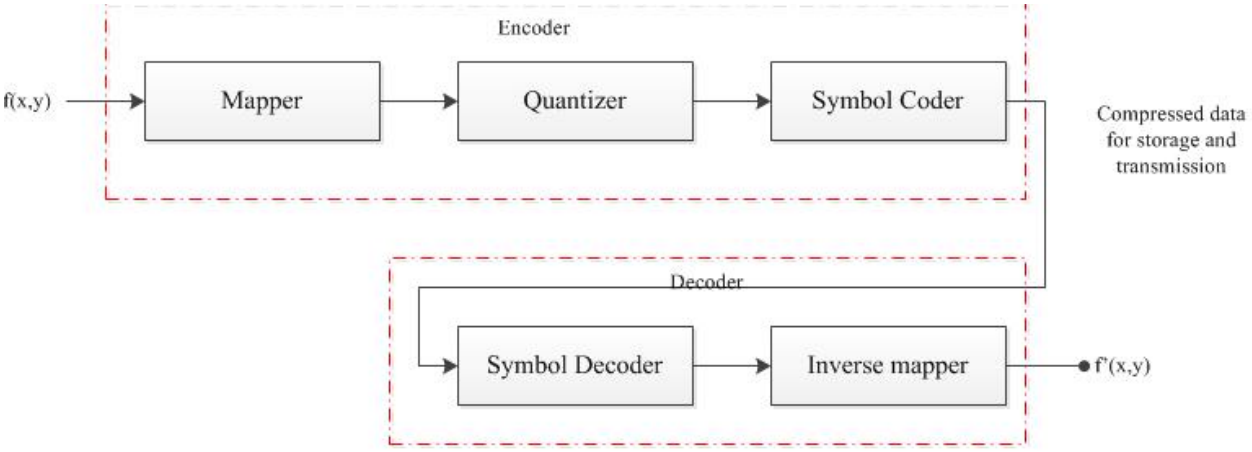

FIGURE 3.3: Image Compression Model

The encoding compression process is elucidated here, the encoder in Fig 3.3 is designed to remove the redundancies through a series of operations.

- **Mapper:** Transforms the *f(x,..)* into a format that reduces both spatial and temporal redundancy. In general, mapping yields the first step of encoding process. The mapping of an image into a set of less correlated transform coefficients.
- **Quantizer:** It reduces the accuracy of the mapper's output in accordance to the pre-established fidelity criteria. As the process is irreversible, it is omitted in application where loss less compression are employed.
- **Symbol Coder:** It generates the fixed-length code to represent the output of the quantizer and maps the output in accordance with the code.

  The decoder in Fig 3.3 contains only two components namely, a symbol encoder and an inverse mapper. They perform the exact inverse operation of the compression system. As the quantization results in the irreversible information loss, we don't include in the reconstruction process and is not included in the decoder model.

3.6 Approach types

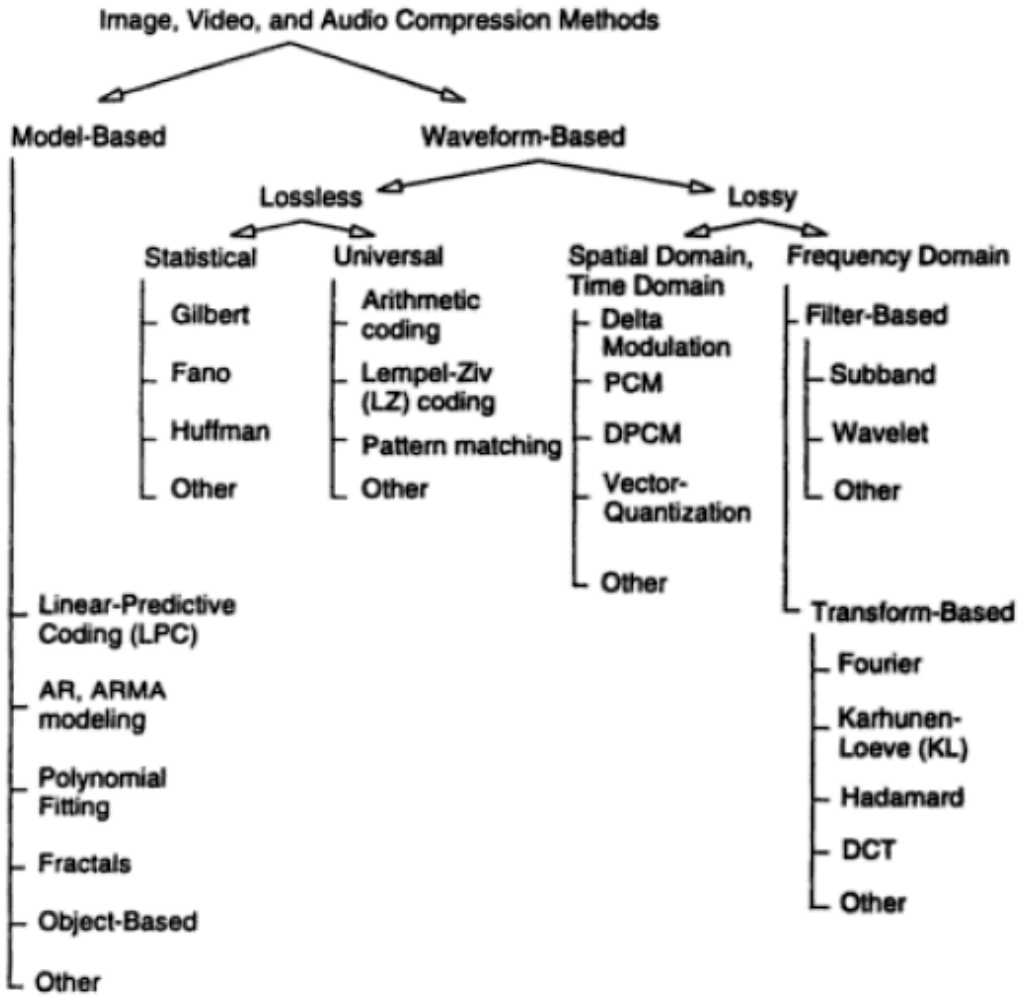

FIGURE 3.4: Various compression techniques [2]

Fig 3.4 represents the classification of compression techniques of audio, video, and image data. Most of the methods are waveform based. For image compression, the two most widely used techniques are lossy and loss less compression techniques. Hence the subsequent sub-sections discuss lossy and loss less compression techniques

TABLE 3.1: Loss less compression Vs Lossy compression

Loss less Compression	**Lossy Compression**
Compression involves in exact replica of the original data.	Compression involves in approximate reconstruction when decompressed the original data. Produces imperceptible losses called as *visually loss less*
No Loss of quantitative information	Loss of quantitative information
Compression ratios are typically low, hence require higher bit rates for transmission	Higher compression ratios can be achievable, requires low bit for transmission, but introduce artifacts.
Examples of usage: Medical data archiving, text documents archiving where single errors can damage the content a lot.	Mostly used in music and natural images, used in cases where the errors are tolerable.

3.6.1 Error Metrics for Lossy Compression

For an original image A (x,y), the decompressed is given by A' (x,y) where M, N are the dimensions of the images respectively. Mainly two of the error metrics used to compare the various compression techniques are Mean Square Error (MSE) and the Mean Square Signal to Noise Ratio (SNR_{ms}). MSE is the cumulative square error between the compressed and the original image and is given by

$$\text{MSE} = \frac{1}{MN}\sum_{x=1}^{M}\sum_{y=1}^{N}[A(x,y) - A'(x,y)]^2$$

(SNR_{ms}) is a measure of the signal to the noise. For our case, we consider signal as the original image and noise to the error in reconstruction of the image and is given by

$$(\text{SNR}_{ms}) = \frac{\sum_{x=1}^{M}\sum_{y=1}^{N}A'(x,y)^2}{\sum_{x=1}^{M}\sum_{y=1}^{N}[A(x,y) - A'(x,y)]^2} \quad (3.7)$$

A compression scheme having the lower values of MSE and higher SNR is considered to be the better one.

According to CCSDS recommended standards, data compression algorithm applied to 2D digital spatial image data from payload instruments.

3.6.2 Discrete Wavelet Transform based compression

The current recommended standard makes use of a three-level, two dimensional (2D), separable Discrete Wavelet Transform (DWT) with nine and seven taps for low- and high-pass filters, respectively. Such a transform is produced by repeated application of a one-dimensional (1D) DWT. Two specific 1D wavelets are specified within this standard: [4]

1. The 9/7 bi orthogonal DWT, referred to as '9/7 Float DWT'
2. The '9/7 Integer DWT' which is non-linear, integer approximation to the earlier.

While the Float DWT generally exhibits superior compression efficiency in the lossy domain, only the Integer DWT supports strictly loss less compression. Both the compression schemes are assumed to use R-bit resolution, $[R \leq 16]$.

The values output from the 3-level 2D DWT are converted to appropriate integer values before applying the Bit Plane Encoder. Each integer is represented using a binary word consisting of a single sign bit along with several magnitude bits. The maximum word size necessary to store each such integer depends on R. Whereas in case of, the computed wavelet domain values are rounded to the respective nearest integers before applying the BPE. A corresponding word length of R+5 bits is adequate to store these integer values. In the case of the Integer DWT,the computed wavelet domain values are multiplied by integer weights that are uniform in each sub band. A corresponding word length of R+4 bits is adequate to store such integers before the weighting factors are applied. [4]

In our Project, we consider the 9/7 Float transform further for compression of the satellite images.

3.6.2.1 9/7 Float Transform

The 9/7 Float DWT uses two sets of analysis filter coefficients ('taps'), the numerical values of the filter taps are given in the table 3.2 along with their representations.

TABLE 3.2: Filter Coefficients for 9/7 Float DWT [4]

i	Lowpass Filter h_i	Highpass Filter g_i
0	0.852698679009	-0.788485616406
±1	0.377402855613	0.418092273222
±2	0.110624404418	0.040689417609
±3	0.023849465020	0.064538882629
4	0.037828455507	-

3.6.2.2 Inverse 9/7 Float Transform

The inverse 9/7 Float DWT uses two sets of synthesis filter coefficients,the numerical values of the filter taps are given in the table 3.2 along with their representations.

TABLE 3.3: Filter Coefficients for 9/7 Float DWT [4]

i	Lowpass Filter q_i	Highpass Filter p_i
0	0.788485616406	0.852698679009
±1	0.418092273222	0.377402855613
±2	0.040689417609	0.110624404418
±3	0.064538882629	0.023849465020
4	-	0.037828455507

3.6.3 Single-Level Two-Dimensional DWT

Image de-correlation is accomplished using a two-dimensional DWT,by iteration of 1D DWT. Viewing the image as a data matrix consisting of rows and columns of signal vectors, a single-level 2D DWT shall be performed on the image in the following two steps in the following order:

1. 1D DWT shall be performed on each image row, producing a horizontally lowpass and a horizontally high-pass filtered intermediate data array, each half as wide as the original image array, as illustrated in Fig 3.5 (b).
2. the 1-d DWT shall be applied to each column of both intermediate data arrays to produce four sub bands as shown in Fig 3.5 (c).

Each of the four sub band data arrays obtained is half as wide and half as tall as the original image array. In illustrations, these sub bands are often shown arranged as one array which has the same size as the original image array, refer Fig 3.5 (c). Starting at the upper left and proceeding clockwise in Fig 3.5 (c), the four sub bands are referred to as LL, HL, HH, LH. [4]

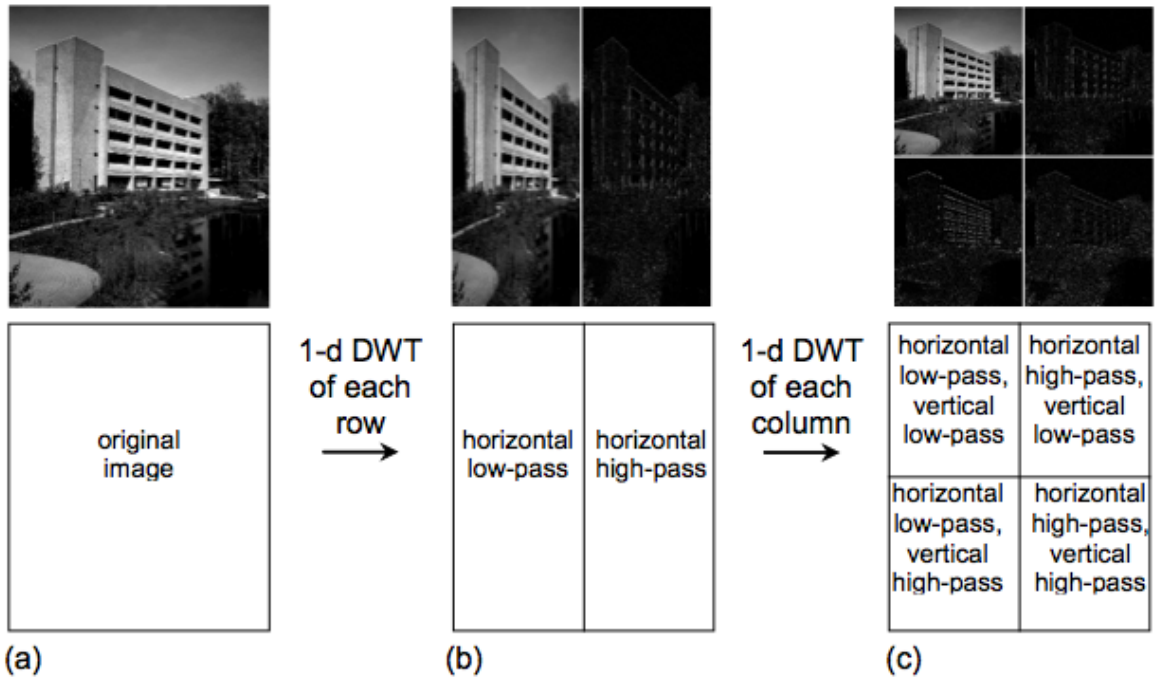

Figure 3.5: 1D DWT

3.6.4 Multi-Level Two-Dimensional DWT

In order to increase the effectiveness of the compression, we can apply further levels if DWT decomposition and eliminate the correlation remaining in the LL sub-bands after DWT decomposition. According to CCSDS, the recommended levels of decomposition is three. This type of decomposition can be explained by the Fig 3.6, the LL of the previous level of decomposition is used for further decomposition. Each additional level of decomposition thus increases the number of sub bands by three but leaves unchanged the total number of DWT coefficients used to represent the image data. In general,n levels of 2D DWT decomposition, the total number of sub bands is therefore $3n+1$. [4]

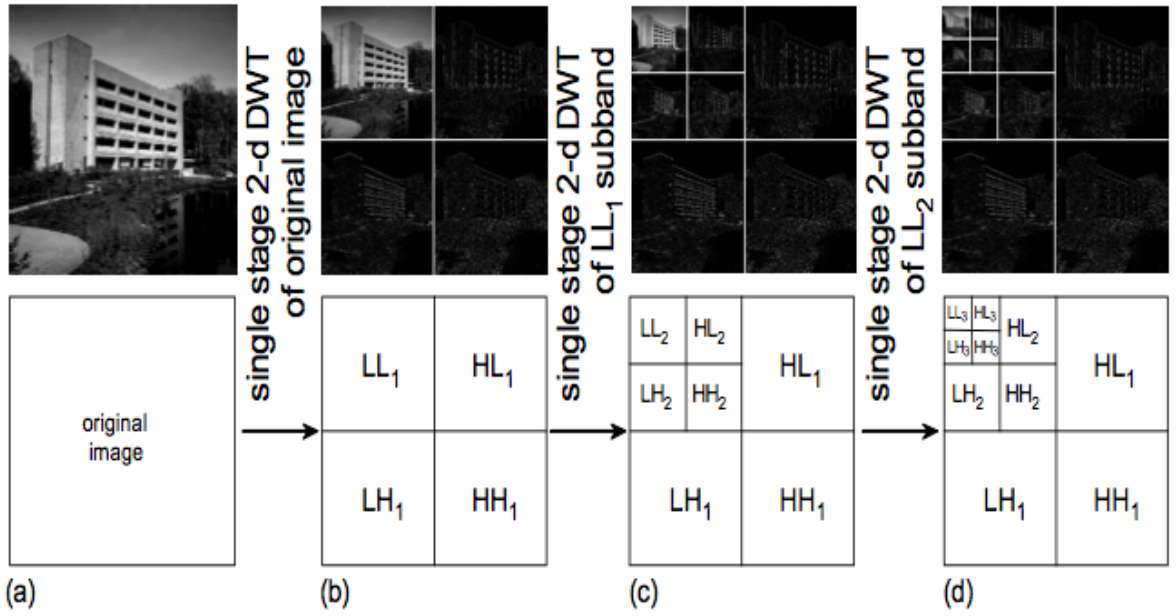

FIGURE 3.6: 2D three level DWT

3.6.5 Inverse Multi-Level Two-Dimensional DWT

The inversion of multi-level DWT is carried out in the following steps sequentially.[4]

1. The four sub bands of highest level, LL3, LH3, HL3, HH3, shall be inverted using an inverse single-level 2D DWT to yield the single sub band LL2, which then replaces the higher-level sub bands in the transform data matrix.
2. The four sub bands LL2, LH2, HL2, HH2 shall be inverted to yield the single sub band LL1, which again replaces the higher-level sub bands in the transform data matrix.
3. A final single-level 2-d inverse DWT shall be applied to sub bands LL1, LH1, HL1,HH1 to reproduce the original image.

3.6.6 Results of compression

Various images have been tested with the implementation of the compression algorithm and best results are documented in the table 3.4 here.

TABLE 3.4: Results of the compression

Parameter	**Original Image**	**Compressed Image**
Row Size	512	512
Column Size	768	768
Compression ratio for 1-Level(%)	1	27.0805
Compression ratio for 3-Level(%)	1	50.1201

FIGURE 3.7: Original test image

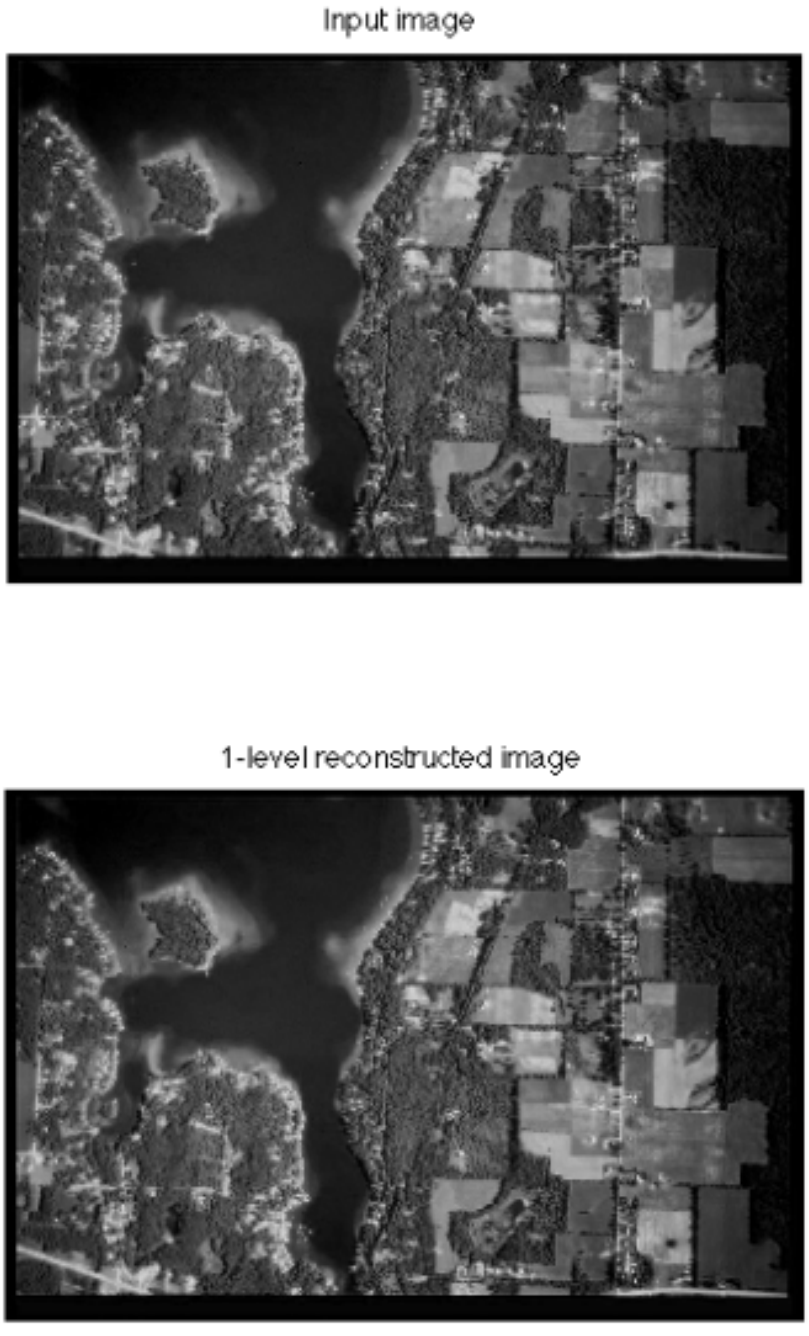

FIGURE 3.8: Result one level 2D DWT compared with Original Image

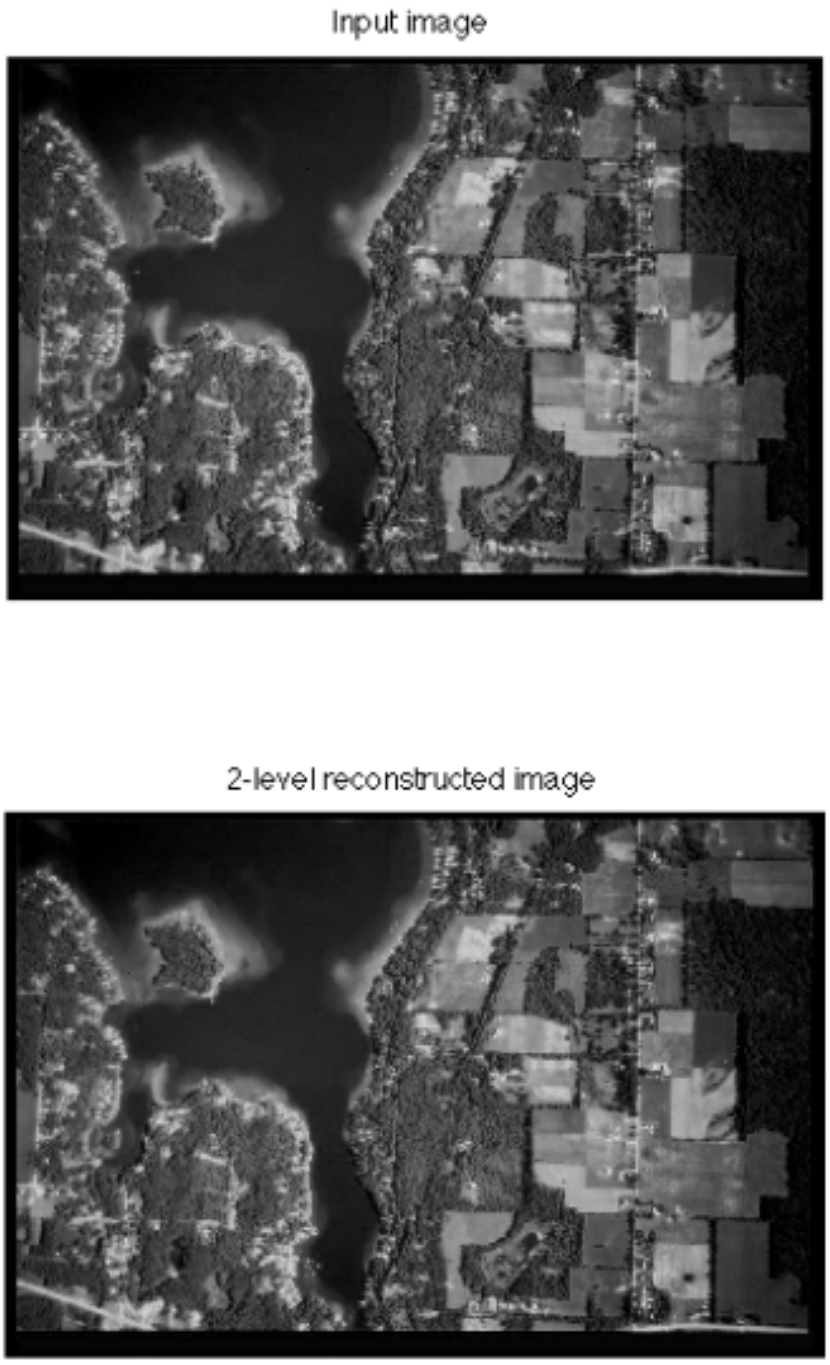

FIGURE 3.9: Result two Level 2D DWT compared with Original Image

FIGURE 3.10: Result three level 2D DWT compared with Original Image

Chapter 4

Firmware Development

4.1 System Configuration

The Vision Payload of Nano Satellite VELOX - I, comprises of a radiation hardened CMOS image sensor which works in array mode. Pixel arrangement in this mode size are given in the table 4.1. In array scan mode, pixels are arranged in 768 x 512 pattern can be seen in the Figure below 4.1

Parameter	**Type**
Operational Mode	Array Mode
Pixel Size	6.5 μm x 6.5 μm
Pixel Array	768 x 512

TABLE 4.1: Operational Mode

The image captured using the above sensor depends on the different parameters slated in the table 4.2 given below.

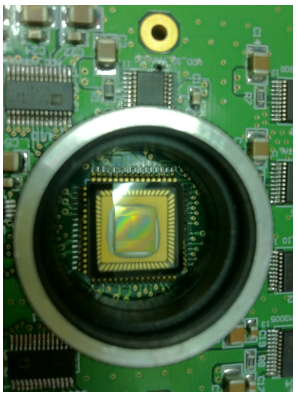

FIGURE 4.1: Image Sensor Board

Quantity	Description
Exposure time	Time for which light is exposed to the pixels. Exposure times are directly proportional to pixel output.
Readout time	Time in which output is read from all the pixels.
Gain	The amplification factor for the voltage perceived before processing.
V_{ref}	V_{ref} values at ADC conversion phase, right balance between the values avoids image extreme darkening / brightening of the image

TABLE 4.2: Sensor Parameters

In order to capture the image from the Payload, two main arguments are to be passed via serial interface ie., they are the slot ID to which the captured files are stored in the SSD memory and the mode of operation of the payload. The first and foremost argument is slot ID. slot ID 254 and 255 are not taken as arguments, these are reserved for specific purposes. One for the random image creation to test the payload functionality and the later to the standard image stored at the time of integration & assembly. Second most important parameter is the mode of operation of the Payload. The mode of operation depends on whether Vref is zero or not. For the true condition, payload is auto calibrated otherwise image is captured. After successful completion of either conditions, function returns to the main and waits for the serial command.

4.2 Programming Essentials

In order to program and execute the Payload firmware, it is to be checked whether the shared libraries are copied into proper location *usr/lib*. Device acceptance rules for FPGA module should be reloaded with commands as in Appendix B. The Linux installation requires the addition of one file to the directory:
`60-opalkelly.rules -----> /etc/udev/rules.d/`

This file includes a generic udev rule to set the permissions on all attached Opal Kelly USB devices to allow user access. Once this file is in place, you will need to reload the rules by either rebooting or using the following `command:`
`/sbin/udevcontrol reload_rules`

With these files in place, the Linux device system should automatically provide write permissions to XEM devices attached to the USB.
For usage of Java API in Linux,

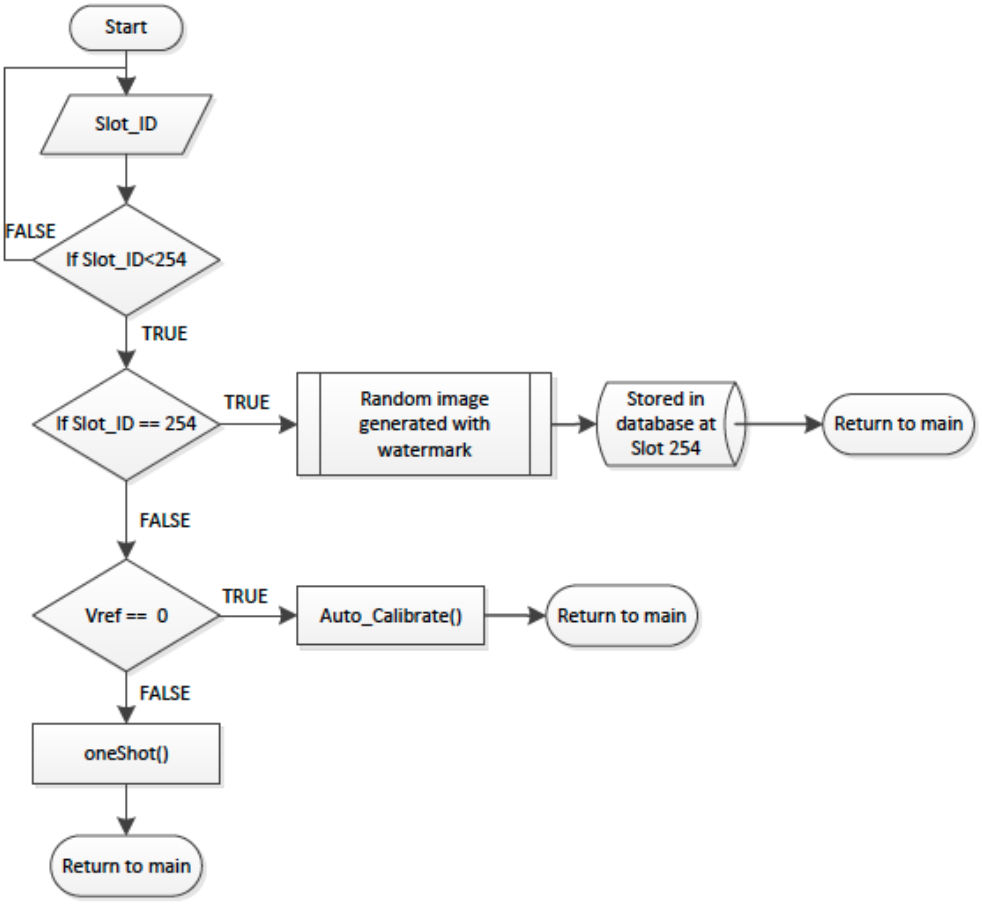

FIGURE 4.2: Top Level Flow diagram

`libokjFrontPanel.so` needs to be copied to the `java.library.path`.
On Debian, you can copy it to `/usr/lib/jvm/jre/lib/i386`

`okjFrontPanel.jar` should be added to your CLASSPATH. It can either be uncompressed or referred to directly on the `javac/java` command lines as below.
To build and run ImageAcquisition.java:

```
javac -classpath okjFrontPanel.jar ImageAcquisition.java
java -classpath .:okjFrontPanel.jar ImageAcquisition e inputfile outputfile
```

The class diagram for the entire payload firmware is as shown in the Figure 4.3

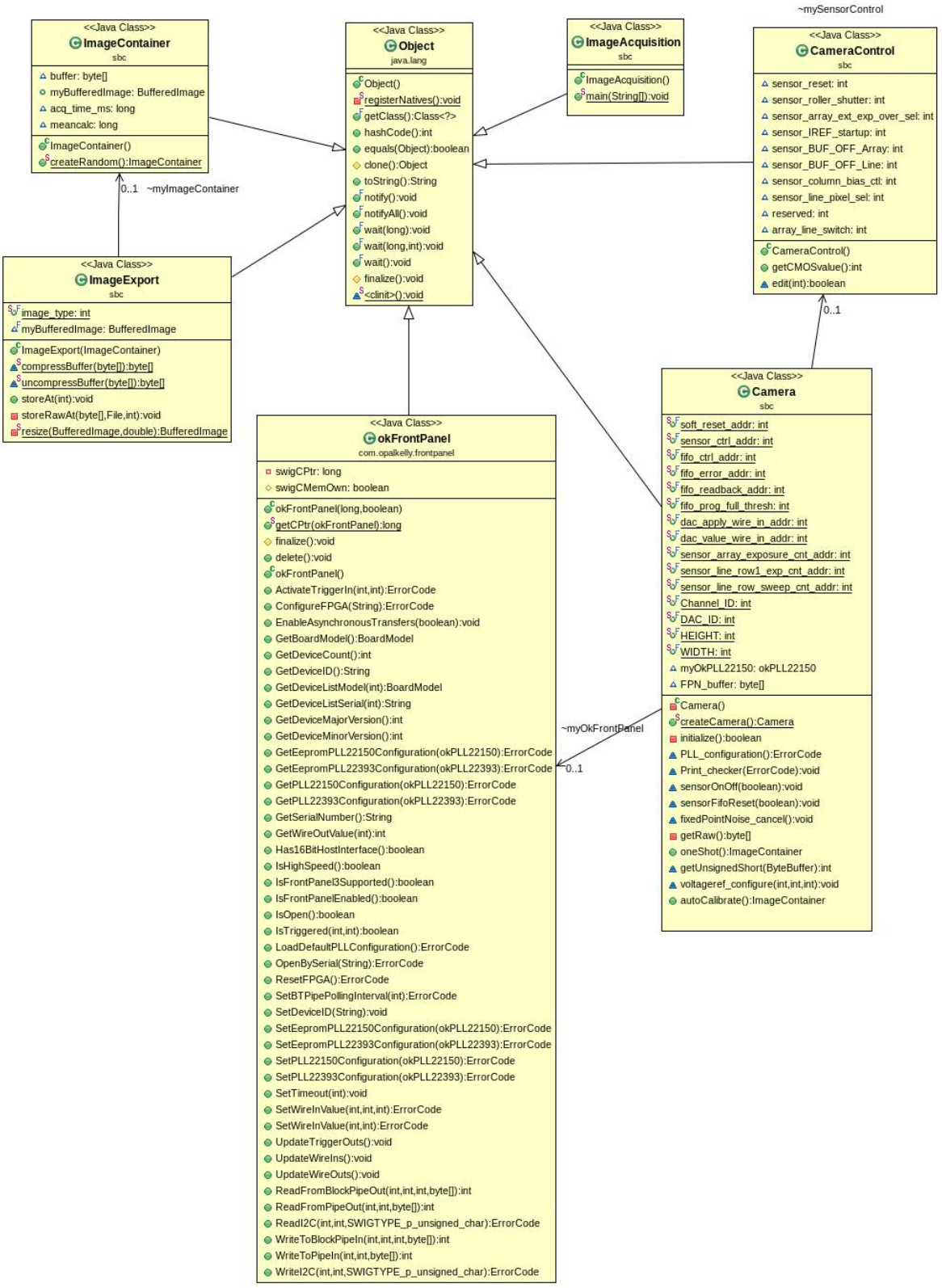

FIGURE 4.3: Class diagram for Payload Firmware

4.3 System Reset

Performs a *reset* of the FPGA internals. This requires that FrontPanel support be present in the FPGA design because the *reset* signal actually comes from the FrontPanel Host Interface (application).

```
if (myErrorCode.equals(ErrorCode.NoError))
public static final int soft_reset_addr = 0x0f;
public static final int sensor_ctrl_addr = 0x00;

myOkFrontPanel.SetWireInValue(soft_reset_addr, 0x8000, 0x8000);
myOkFrontPanel.UpdateWireIns();

myOkFrontPanel.SetWireInValue(soft_reset_addr, 0x0000, 0x8000);
myOkFrontPanel.UpdateWireIns();

myOkFrontPanel.SetWireInValue(sensor_ctrl_addr,
mySensorControl.getCMOSvalue(), 0xfffe);
myOkFrontPanel.UpdateWireIns();
```

Wire In endpoint values are stored internally and updated when necessary by calling `(UpdateWireIns()`. The values are updated on every endpoint basis by calling this method. In addition, specific bits may be updated independent of other bits within an endpoint by using the optional mask. This method is called after all Wire In values have been updated using `SetWireInValue()`. The latter call merely updates the values held within a data structure inside the class. This method actually commits the changes to the XEM simultaneously so that all wires will be updated at the same time.

4.4 Payload Initialization

The FrontPanel API provides a powerful C++ interface to Opal Kelly USB boards. To build an application using this API, one should include the files okFrontPanelDLL.h and okFrontPanelDLL.cpp in the project if programmed in C/C++. These files contain stub functions that call to the DLL or Shared Libraries (in case of Linux). In our case, as the application framework is developed in Java on Linux Single Board Computer(SBC), we should also include shared library object files

during run time termed as 'libokjFrontPanel.so' and it is also mandatory to export their path and specify at the time of compilation. To use the library, you create an instance of myOkFrontPanel which encapsulates communication with the USB driver and provides access to FrontPanel endpoints. Initialization is as shown in the Figure 4.4
Firstly, libraries are to be loaded and an instance is created for checking the system error codes by,

```
System.loadLibrary("okjFrontPanel");
ErrorCode myErrorCode;
```

An instance of the okFrontPanel created in the application by,
`okFrontPanel myOkFrontPanel`
`myOkFrontPanel = new okFrontPanel();`

Here, `myOkFrontPanel` will be referred as a class whenever its sub functions are needed to be utilized in the application.
Secondly, the computer needs to scan for the XEM model which it is about to communicate.An empty string variable needs to be declared to store the device serial number, which will be used to open the device. The sequence of commands is:

```
System.out.println("OpenBySerial:" + myErrorCode);
System.out.println("GetDeviceCount:" + myOkFrontPanel.GetDeviceCount());
BoardModel myBoardModel = myOkFrontPanel.GetDeviceListModel(0);
System.out.println("BoardModel:" + myBoardModel.toString());
System.out.println("DeviceID:" + myOkFrontPanel.GetDeviceID());
```

This retrieves the serial number of the first connected device, depicted by the integer '0', and stores it in a string myErrorCode, which will be used in the `OpenBySerial` function of the myErrorCode class. Besides the retrieving the serial number of the device, additional commands are used to retrieve the number of devices connected and their respective board models for the user's reference during application development.

```
BoardModel myBoardModel = myOkFrontPanel.GetDeviceListModel(0);
System.out.println("BoardModel:" + myBoardModel.toString());
```

The command returns an integer relating to the first scanned XEM device, which

subsequently needs to be referred to a lookup table containing the corresponding device models. After storing the data into the variables, appropriate combinations of switch(case) gains access for different functions from the serial interface.
Thirdly, PLL has to be configured with the set the commands defined in the data sheet of cypress semiconductor and the Opal Kelly user manual [8] [14].
Create an instance for PLL by,

```
myOkPLL22150 = new okPLL22150();
myOkPLL22150.SetReference(48.0f, false);
// default PLL settings, Vref=48Mhz, fixed for CY22150
myOkPLL22150.SetVCOParameters(400, 48);
// VCO=48*400/48=400Mhz, DO NOT CHANGE THIS.
myOkPLL22150.SetDiv2(DividerSource.DivSrc_VCO, 20);
// VCO,DIV2N=20.  Div2ByN =400/20 = 20MHz
myOkPLL22150.SetOutputSource(0, ClockSource.ClkSrc_Div2By4);
// 400/4 = 100MHz.  for SDRAM
myOkPLL22150.SetOutputEnable(0, true);
myOkPLL22150.SetOutputSource(2, ClockSource.ClkSrc_Div2ByN);
// Div2ByN =400/20 = 20MHz
myOkPLL22150.SetOutputEnable(2, true); // Div2ByN for exposure clock
// disable other clock outputs
myOkPLL22150.SetDiv1(DividerSource.DivSrc_VCO, 20);
// divider1:  input,VCO,DIV1N=20.  Div1ByN = 400/20=20MHz
myOkPLL22150.SetOutputSource(1, ClockSource.ClkSrc_Div1ByN);
// Div1ByN for main clock (sensor, ADC)
myOkPLL22150.SetOutputEnable(1, true);
myOkPLL22150.SetOutputEnable(3, false);
myOkPLL22150.SetOutputEnable(4, false);
myOkPLL22150.SetOutputEnable(5, false);
return myOkFrontPanel.SetPLL22150Configuration(myOkPLL22150);
```

Finally, a configuration file is loaded into the FPGA. This configuration file is generated from the Xilinx ISE software, which contains the digital blocks programmed in VHDL.

```
myErrorCode = myOkFrontPanel.ConfigureFPGA("get/bin/top.bit");
```

The above example loads the configuration file named ‘top.bit’ into the FPGA. This also returns an integer value which indicates whether the configuration is

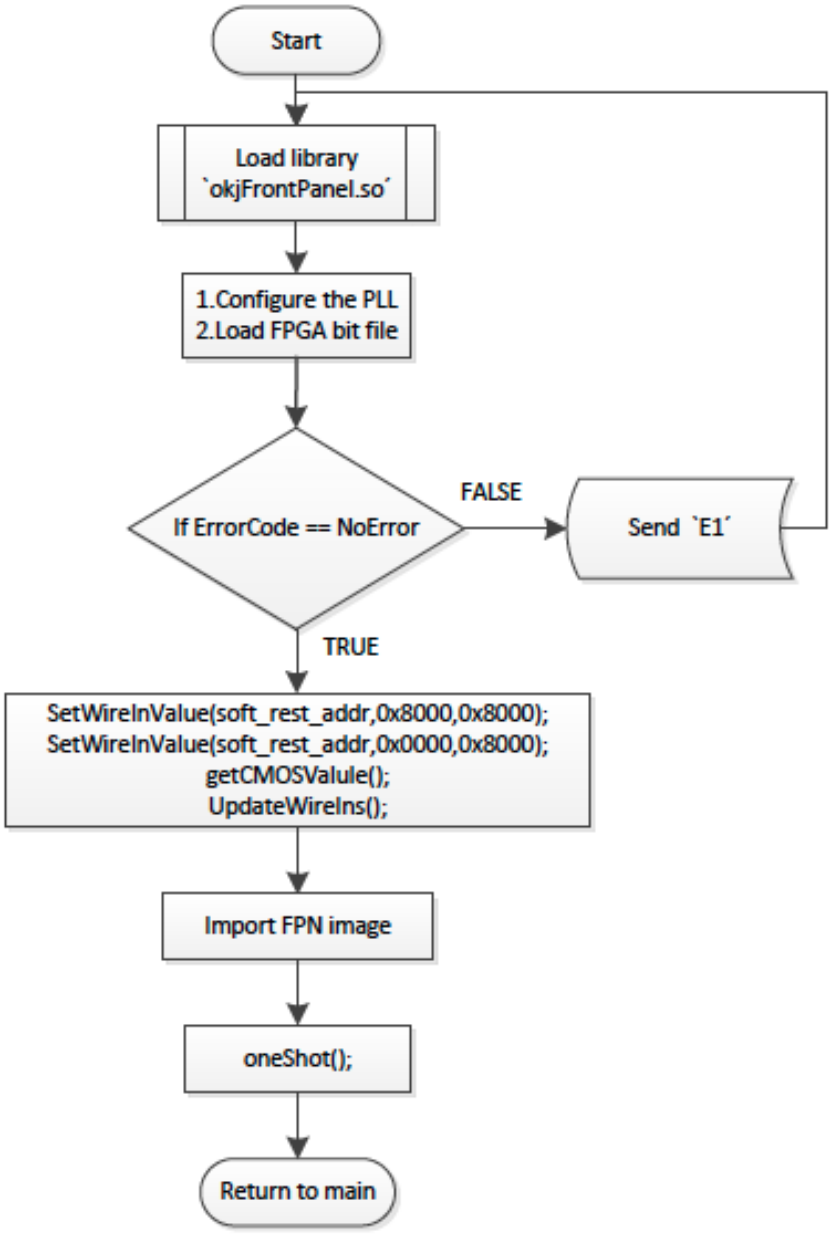

FIGURE 4.4: Payload Initialization

successful. For a no error case, the returned value is 0.

4.5 Configurable Payload Parameters

The Payload can be configured with variable key parameters that effect the image quality, list of such parameters are shown here. These parameters can be configured via UART serial interface protocol defined in the Chapter 6 in this thesis.

TABLE 4.3: Clock Values selection

Register Value	**Effective Frequency [MHz]**
30	13.333333
31	12.903226
32	12.5
33	12.121212
34	11.764706
35	11.428572
36	11.111111
37	10.810811
38	10.526316
39	10.256411
40	10.0

These parameters are configured with arguments (min,max,value) and some typical values for test have be shown here as an example.
array_exposure_cnt(0, 1023, 1023),
main_clk(1, 40, 25),
exposure_clk(1, 40, 31),
cds_gain(0, 3, 1),
probe_select(0, 1, 1),
vref(0, 255, 127),
stretch_lo(0, 4096, 506),
stretch_hi(0, 4096, 2956);

These parameters are once initially configured in the from the serial interface later on the configuration is stored in '*campar.bin*' and accessed whenever the configuration is changed depending on the region of interest that is to be captured.

4.6 Main and Exposure Clocks

The main clock provides the timer to the FPGA. Clock register value determine the quality of the image and for this sensor they are observed in the range of 30-40. We perform the following experiment: The lens is covered with a lid to prevent the exposure of the CMOS sensor to light. Then, we sweep through all possible pairs of clock values, taking 20 exposures for each tuple. We average the images for each clock value tuple and form the distribution of gray-scale values, as well as correlation of adjacent pixels.

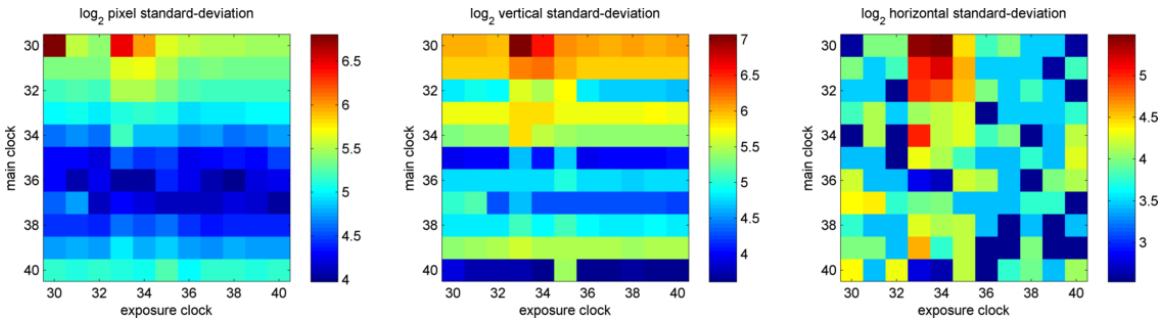

FIGURE 4.5: Black Standard deviation

The results are shown in Figure 4.5 and Figure 4.6. The noise distribution varies significantly with the choice of clock values.

- To minimize the pixel noise variance, the main clock register should range between 35 - 38.
- To maximize the correlation of the vertical adjacent pixels, the main clock register should be set to 35, 37, or 40.
- To maximize the correlation of the horizontal adjacent pixels, the main clock and exposure clock values can be selected from the list: (35,32), (36,38), (37, 40), (38, 39), (39, 37), ..., (40, 36).

For our final algorithm, we combines these rules of thumb. We have distilled a list of clock value register tuples that the exposure mechanism chooses randomly from. In the firmware (40, 39), (39, 34), (39, 32), (37, 40), (37, 39), (37, 38), (37, 32), (36, 40), (36, 39), (36, 38), (36, 37), (36, 36), (35, 32).

4.7 Exposure time

Exposure time has the great impact on image quality as they affects the contrast of an image. Typically, an image with good contrast values has a spread distribution of gray-scale values.

- If the exposure time is too small, the image exhibits mostly dark pixels.
- If the exposure time is too large, the image exhibits mostly white pixels

In order to obtain an image with good contrast, the exposure time needs to be chosen just right. The exposure time does not relate to average intensity, i.e. mean gray-scale, in a linear fashion. Our experiments suggest, that for each scene, there is a region on the exposure time logarithmic scale, where the average intensity increases linearly. Once the average intensity approaches a limit, it does not increase significantly anymore.

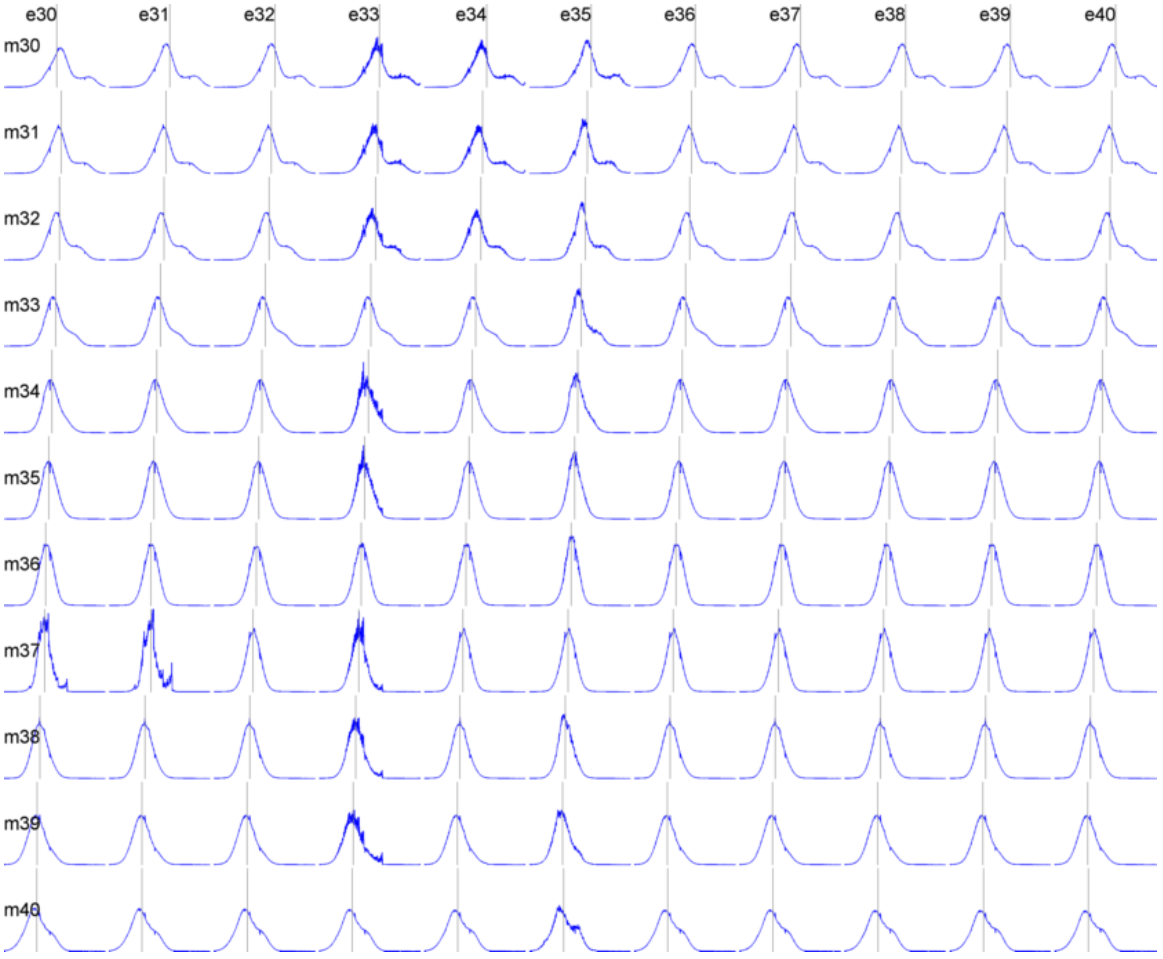

FIGURE 4.6: Black Standard deviation

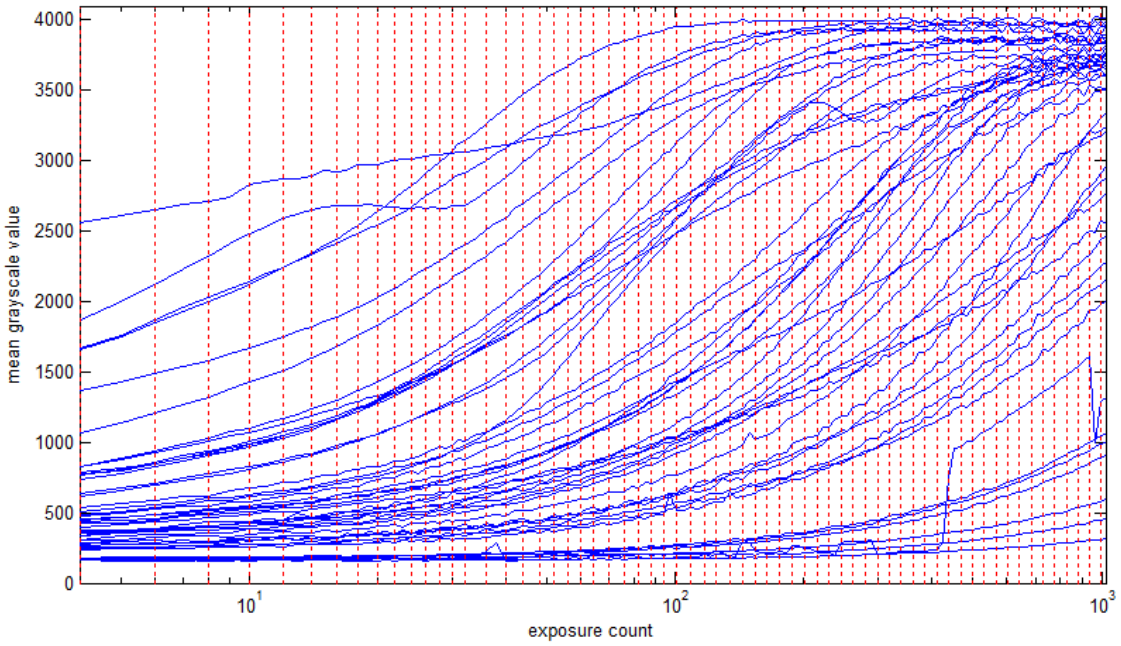

FIGURE 4.7: Exposure time Vs mean gray-scale

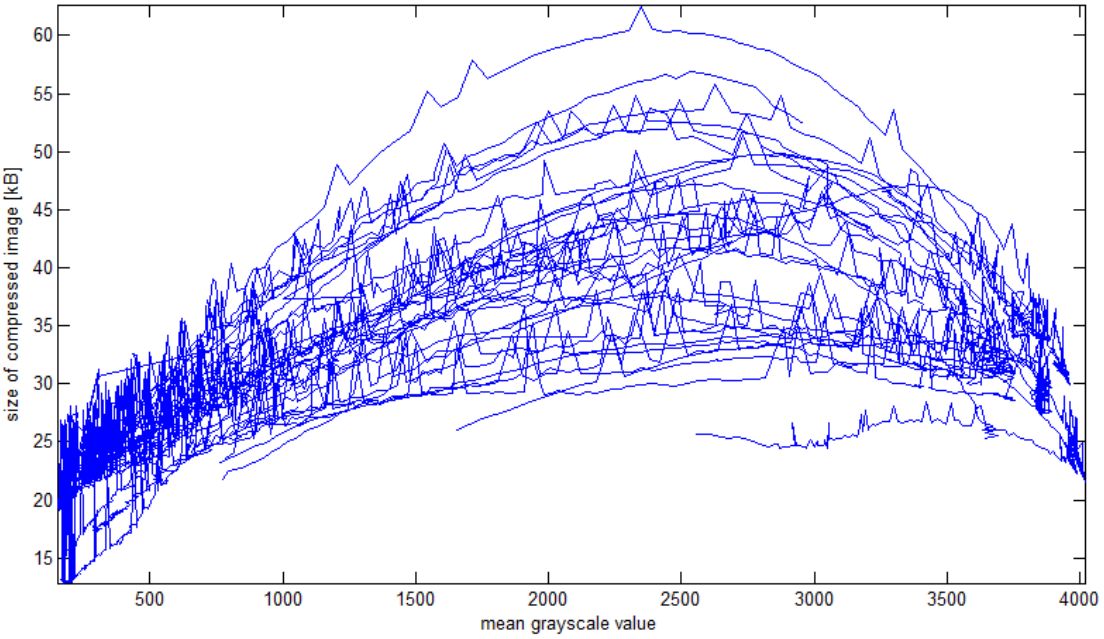

FIGURE 4.8: Mean gray-scale Vs compressed image size

Above, we mentioned that the average intensity should ideally be medium gray. In order to back that claim, we evaluate the file sizes of the images in their compressed format. A low file size means, little information remains in the image, when compared to an image of the same scene with a larger file size. Our experiments suggest that the maximum file size is not obtained at the exact medium intensity, i.e. 50% gray-scale, but above that value namely around 60% gray-scale value. The results of this observation can be shown in Figures 4.7 and Figure 4.8.

4.8 GUI development

Graphical User Interface is developed in order to experiment the Sensor quality and faster configuration of key parameters. Images are captured at different instants with varying configurable parameters. Screen shot of the GUI developed can be seen in the Figure 4.9. The sliders in the GUI with key configurable parameters can be adjusted to their (minima,maxima) limits programmed earlier.

4.9 Image Acquisition

During the sensor configuration, the configurable parameters stored in *campar.bin* are stored in global variables. For the Readout and Exposure clocks, the respective PLL [14] will be configured immediately after the file is parsed and read.

FIGURE 4.9: GUI for Vision Payload

These parameters are sent to the FPGA for configuration. These variables will be processed in various sub functions in the program, before sending the updated configuration parameters to the FPGA The image acquisition operation can be performed anytime after the successful configuration of the sensor & FPGA. Taking reference from the these values, sensor configuration is set and the corresponding image with respect to the mode of operation and number of slot to store the captured image is processed. Next, the data for the Fixed Pattern Noise (FPN) is loaded and stored in an FPN buffer *myByteBuffer2*, details on how the FPN values are obtained will be discussed in the later section. The digitized raw data of the image is then read from the SDRAM and stored in another buffer *myByteBuffer* using the `ReadFromBlockPipeOut()` function explained earlier. Noise cancellation of the data is performed by subtracting the FPN values from the obtained raw data and the new image without noise is obtained. As these values are in 12 bits, the operations have to be done on a high byte and a low byte, which requires 2 elements for both arrays. Thus bit shifting operations and address assignments to the values have to be performed during the noise cancellation. In addition, the obtained values after noise cancellation cannot be outside the 12 bit (0-4095) range. These values will be set to the corresponding minimum or maximum values. The algorithm is shown below, where by a for loop is called with the number of pixels set as a loop count (c0) limit . The retrieved values from the FPGA, stored in myByteBuffer, is being subtracted with the myByteBuffer2. The higher bytes of the 2 arrays are multiplied by 256, which is equivalent to an 8 bit left shift, while the lower bytes are kept at their original value. After the computation, the final value is stored in the variable myInt, which will be processed to set all

values below 0 to be 0, and values above 4095 to be 4095. Finally, the individual buff_val will be separated into 2 bytes, storing them at 2 separate locations in the sdram_buffer array. Appropriate masking and bit shifting operations are used to ensure the values are correct.
After the noise cancellation operation, the data is further mapped into 8 bits using a set of limits. Similarly, the values outside the limits will be set to either 0 or 255, while the rest will be normalized to their equivalent 8 bit value. The algorithm shown below processes the similar buff_value obtained earlier. The 8 bit normalization limits are determined by global variables *strech_lo* and *strech_hi*, whereby values exceeding the limits will be set as 0 for the lower limit and 255 for the upper limit. The values within range will be normalized by proportion. The arrays which contain the image information will be subsequently saved in a binary format file.

After Successful initialization of the Payload, a raw image is stored in the myByteBuffer via routine getRaw(). A condition is introduced to check whether the image is created or not, TRUE succeeds importing of FPN buffer image to the myByteBuffer2. New image is produced after cancellation of the Fixed Pattern Noise. Further image is down scaled from 12 bit resolution to 8 bit and stored in the external folder *Image Container* in our case for further operations on board of the satellite like thumbnail creation, compression, filtering etc., Process can be explained with the control flow diagram in 4.10.

4.10 Fixed Pattern Noise Cancellation

The FPN noise is the pixel noise generated when the camera is in operation, whereby particular pixels are susceptible to giving brighter intensities above the general background noise. The pixel layout of the camera sensor forms patters of 16 columns of pixels, which resulted in a pattern of vertical lines appearing on the image. After applying a reference setting (Readout Clk, Exposure Clk, Array Mode Exposure Count) on the camera, the FPN noise is captured when the aperture of lens is closed and saved for further processing in removal of the noise. Vref is adjusted such that the digitized values of the pixel noise are not too high or too low to perform noise cancellation. If the noise values are too high for noise cancellation, an image will not be formed due to the low resultant bit values after cancellation. If the noise values are too low, the vertical lines will still be visibly prominent in the image. The mean of the digitized 12 bit voltage is monitored in the GUI upon image capture. white piece of paper is used as an image reference to determine whether the noise is still visible after noise cancellation.Fixed pixel bias

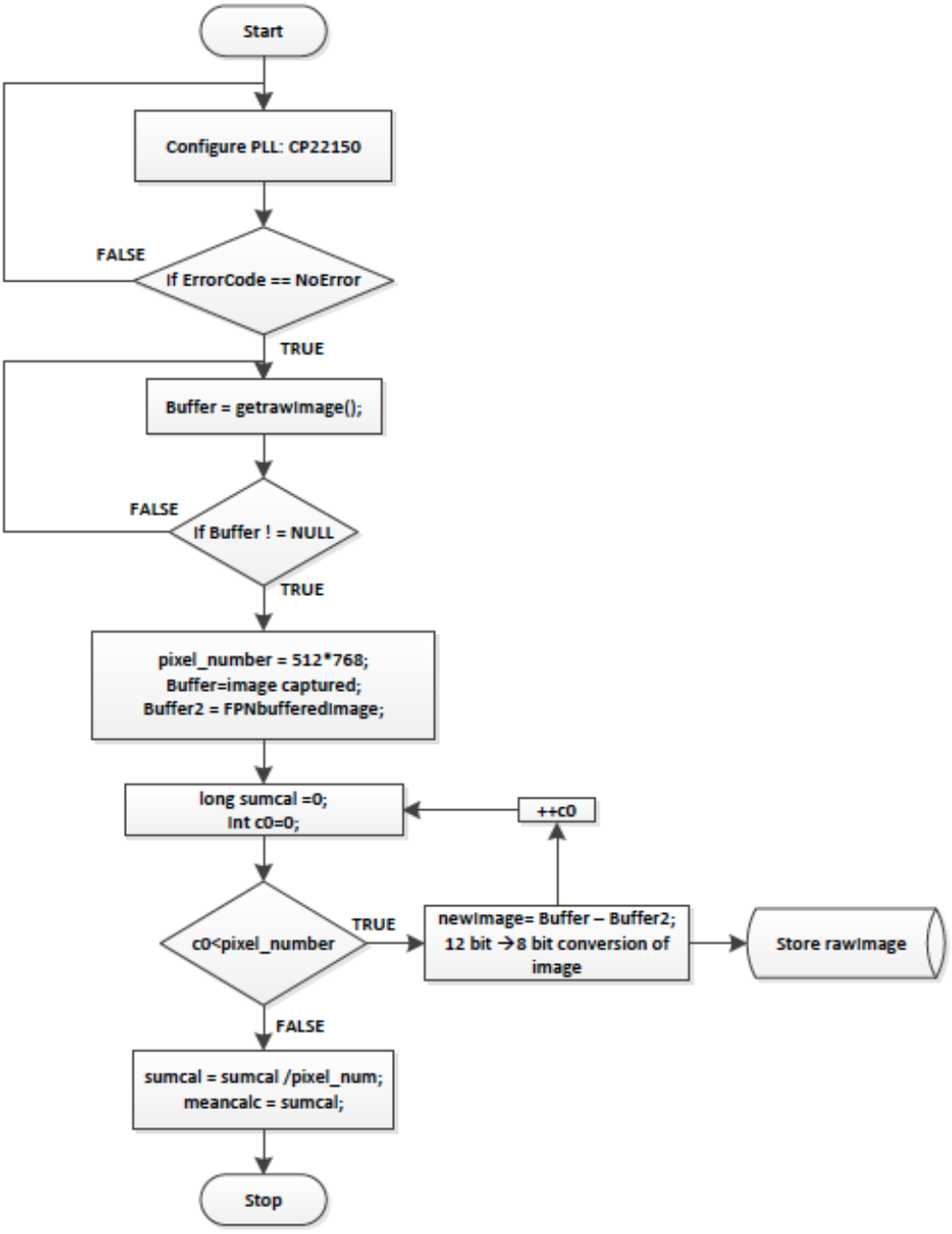

FIGURE 4.10: Image Acquisition

denotes the average intensity perceived by the pixel location when the exposure occurs in total darkness. In total darkness, all pixels should ideally read out identical values (since the light intensity is the same for all pixels). However, due to irregularities in manufacturing, each pixel and in particular each column has it's own characteristic bias. The bias can be established by taking a great number of images in total darkness and averaging the captured intensities. The pixel bias does not notably change over time and is therefore called fixed bias. Moreover, the bias is added to the pixel regardless of intensity. That means, once the pixel bias is established, it can be subtracted from a regular exposure to significantly improve imaging quality.

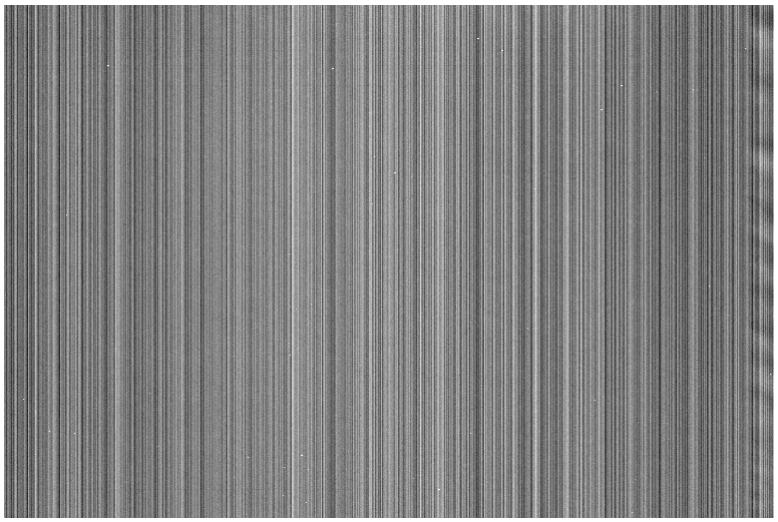

FIGURE 4.11: Recorded FPN from the Sensor

4.11 CMOS Sensor Calibration

4.11.1 Manual Calibrated Settings

There are 2 ways of configuring the settings manually. The first method is to input the parameters sequentially in the program, which maybe troublesome and prone to errors if the parameters are entered in the incorrect sequence. The second method is to load the settings from a text file, which is more reliable as all the parameters will be loaded in the same time and these details can be checked on ground before sending the data to the satellite. That is how we have the '*campar.bin*' for every best capture of the image stored. We can retrieve the settings from the file whenever needed.

4.11.2 Auto Calibration Settings

Auto Calibration routine can be explained with the help of control flow diagram as shown in 4.12

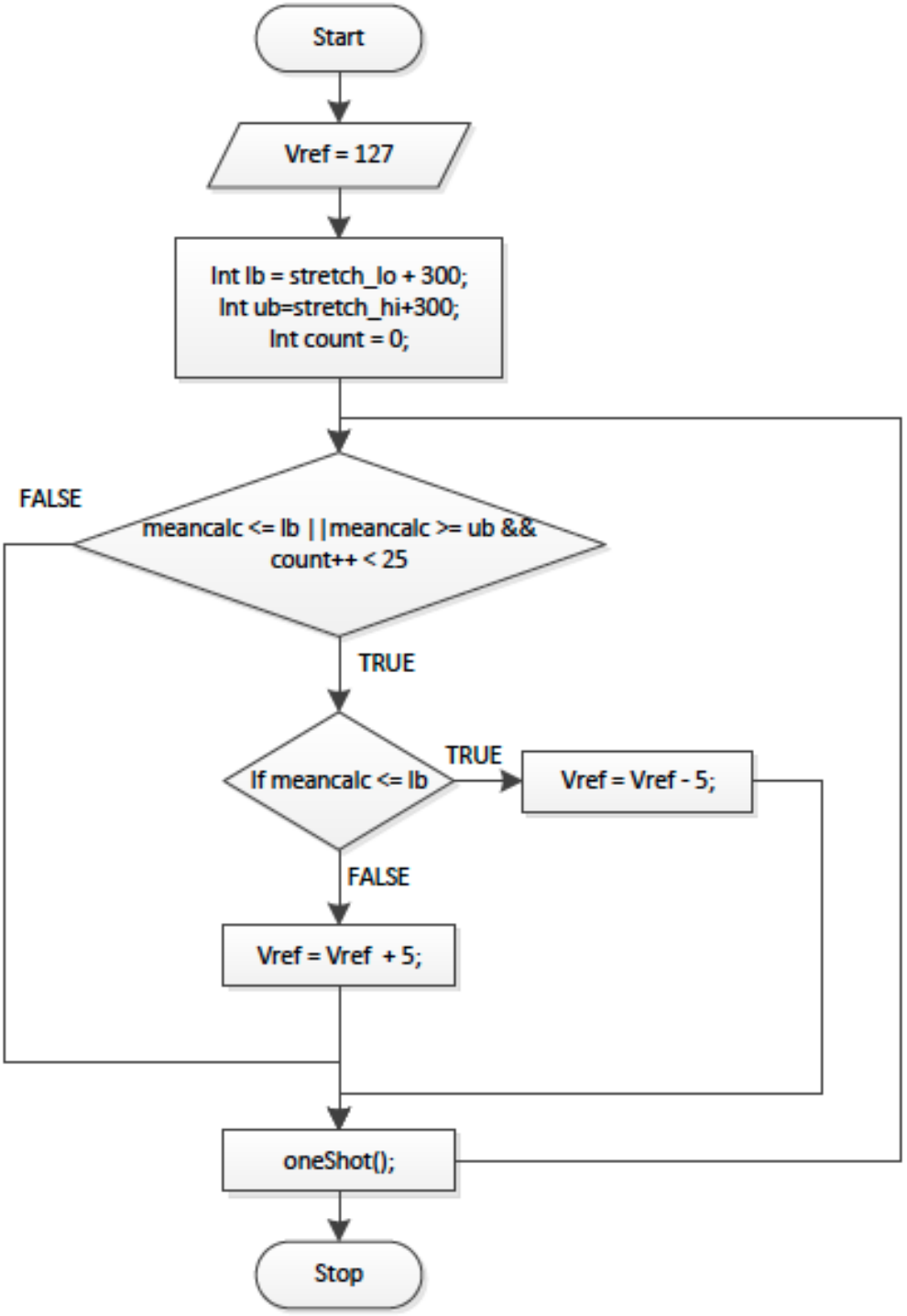

FIGURE 4.12: Auto Calibration

The auto calibration feature was added to increase reliability to the performance of the vision payload. After the launch of the satellite, manual calibration of the camera will be very tough and inefficient, as sampled images can only be sent to the ground station at hourly intervals and lighting conditions in space cannot be simulated on ground. Therefore, if the camera is able to perform a self calibration and send a visible raw image back to the ground station, image processing can be done on ground in order to improve the quality of the captured image. It should be noted that this auto calibration is only done for the array mode function. As explained earlier, the critical parameter to be adjusted is Vref as it determines whether an image can be captured. To ensure that majority of the pixel voltage values are being sampled within the ADC range, the mean of the digitized values have to be calculated. A low mean close to 0 signifies that the pixel voltage values are mostly below the sampling range of the ADC, thereby a lowering of Vref is required. The same principle can be applied to the opposite bit limit at 4095. A suitable mean value will be approximately 2048, which is in the middle of the digital range of the ADC. Hence, the algorithm of the auto calibration involves sampling image frames which returns the mean value of the digitized voltage. As long as the mean does not fall between a suitable range, Vref will be increased or decreased and a frame is captured again.

The other parameters such as the readout time, exposure time, sensor gain and array exposure count can be set manually from serial interface by the user or be loaded from the pre-saved configurations. This has to be done as different exposure times at different 64 environmental conditions will produce different image results. For example, if the exposure time is set for too long in a bright environment, this will cause majority of the pixels in the frame to output a high voltage, which makes the image appear too bright at most of the sections. After all these parameters have been set, the program will proceed with the Vref auto calibration.

The main algorithm for the auto calibration is shown in 4.12. The global variable meancalc stores the mean value of the digitized voltage of the pixels, which is the sum of all the digitized values divided by the number of pixels. A while loop is implemented to keep repeating the operations inside the loop as long as the mean value is outside the specified range, which is from 2000 to 2100. In the loop, the function oneShot() is called to capture an image and update the meancalc global variable. If the mean is outside the indicated range, ADC_value, which is the digitized value of Vref, will be subtracted or added by 25 bits accordingly. In this context, a 25 bit shift is equivalent to a 0.02V shift in Vref. Another stop condition for the while loop is added for cases whereby the Vref is set at its minimum or maximum value when the adjustment exceeds the allowable Vref range. This prevents the computer from sending the wrong digital values to the

ADC which will affect the performance of the camera.

After Vref is set after auto calibration, the buffer limits for the 8 bit normalization is set by using the last maximum and minimum 12 bit digitized voltage recorded during the multiple frame captures for auto calibration. The preview of the image capture with improper exposure settings before auto calibration yields an image like this in Fig 4.13. And after calibration can be seen in Figure 4.14

FIGURE 4.13: Image capture before sensor calibration

FIGURE 4.14: Image capture after sensor auto calibration

4.12 Image Export & database

The number of the slots for the images folder is temporarily restricted to 255 for the convenience in the developed despite of availability of huge memory (2 GigaBytes). After the successful operation of the image acquisition, raw image is stored in the database with the slot ID that is passed as an argument. Simultaneously the raw image is processed to create the required image formats such as thumbnail (re-sized image), compressed raw binary file are achieved.

FIGURE 4.15: Image database structure

FIGURE 4.16: Image database structure expanded for particular slot

Text File information of the image captured is as shown below:

```
date=2012-09-13T12:34:11.747+0800
array_exposure_cnt=890
main_clk=25
exposure_clk=31
cds_gain=1
probe_select=1 vref=127
stretch_lo=506
stretch_hi=506
acq_time_ms=285
```

Chapter 5

Payload Interface Development

5.1 Introduction to Serial Port

The Universal Asynchronous Receiver/Transmitter is abbreviated as UART, which is serial I/O device and is found on any micro-controller or microprocessor. Serial port converts the stream of data between parallel and serial formats, transmits on its output pin and receives on its input pin respectively. The UART takes bytes of data and transmits individual bits in a sequential fashion, the send and receive data between two serial ports includes a mandatory *shift register* which is core for conversion of these parallel and serial streams of data. Serial transmission of digital information (bits) through single wire is more cost effective compared to parallel transmission which needs multiple wires. [15]

5.1.1 Data Flow Speeds & Control

The standard UART clock-frequency for PCs equals to 1,843,200 cycles-per-second. Each data-bit consumes 16 clock-cycles. So the fastest serial bit-rate in PCs would be 1843200/16 = 115200 bits-per-second.

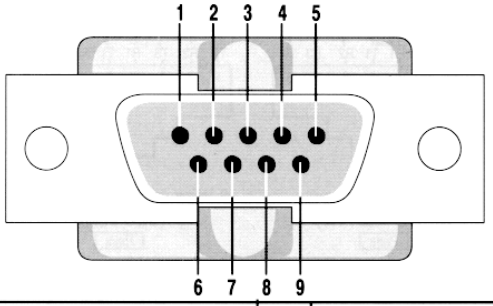

Pin	Signal	Pin	Signal
1	Data Carrier Detect	6	Data Set Ready
2	Received Data	7	Request to Send
3	Transmitted Data	8	Clear to Send
4	Data Terminal Ready	9	Ring Indicator
5	Signal Ground		

FIGURE 5.1: UART Serial [3]

5.1.2 Character Framing

FIGURE 5.2: UART single byte frame

An example standard data frame is represented in the figure 5.2 above, following the conventional way the idle, no data state is held high or powered up. Each data frame is initiated by a start condition which is normally logic low, and ended by the stop bit which is logic high. These start/stop conditions are user configurable and can be of any size. Usually, the logic low at the receiver end and logic high after data frame indicates the complete transfer of the data frame.

5.2 Serial programming for POSIX systems

Serial programming comply with four mandatory operations in sequential order for successful establishment of communication over the serial port. These operations includes opening the serial port, configuring the serial port, read and write bytes to and from the serial port, and closing the serial port when the task has been accomplished. It is significant to check the acknowledgment at each stage to ensure that the task has been completed, because failure may introduce improper data transfer over the terminal and these errors are difficult to trace.
Serial port being bi-directional, shall be able to send/receive data at the same

time which is known as over-lapped communication which requires very complex objects such as threads, mutexes, and semaphores. For my thesis, i have considered only non-overlapped communication. My goal to create a source/header file that provides a consistent interface, that the programmer can only link against the object library for the operating system (Linux). [15]

5.2.1 Opening a Serial Port

The first and foremost step that is necessary to communicate over the serial port is to open the device. Under Linux, the serial port is treated as a file, so however in general the commands used would be similar to opening a file. File handling needs permissions in Linux and they constrained to the particular user in Linux. So as to provide access to particular files one need to grant permission through the root user. Here, in our case the PPU is the root, nevertheless it has all the permissions needed and given if necessary. [15]

```
int fd = open("/dev/ttyUSB0", O_RDWR | O_NOCTTY | O_NDELAY);
//the name of the serial port as a c-string (char *)
eg., /dev/ttys* serial port name * can be 0/1/2/3 anything,
//configuration tty O_RDWR - we need read and write access
//O_CTTY- prevent other input (like keyboard) from affecting what we read
//O_NDELAY - We don't care if the other side is connected
(some devices don't explicitly connect)
O_RDWR | O_NOCTTY | O_NDELAY );
if(fd == -1) {
//Write down the error code
}
```

5.2.2 Configuration the Serial Port

The second operation before data transfer is to appropriately configure the serial port. Port configuration includes parameters like communication speed, data size, parity, flow control and number of stop bits. The communication speed is the speed at which the serial port can transmit and receive data and is specified in units of BAUD. Common speeds are 9600 BAUD, 19200 BAUD, and the current maximum of standard serial ports is 115200 BAUD. Data word size is the size of a piece of the data, usually a word/byte, or eight bits. Parity is the type of parity used, either even, odd, or none, and flow control and the number of stop bits are used to synchronize the communication [15]. It is absolutely mandatory to have same

communication speeds between two UART devices which are intended to communicate. And is also a good practice to maintain time-outs for non-overlapped communication like in our case. Setting these timeouts ensure the efficient way of communication to return failure instead of blocking the communication. For our purpose of the project, instead of using timeout fashion in configuring we expect an acknowledgement to the host after each successful operation/transfer.
Configuring the serial port in Linux uses termios struct, and carried out in the following steps:

1. Create the struct and initialize the current port settings.
2. Set the speed attribute of the struct to the desired port with the functions cfsetispeed() and cfsetospeed(). Note that both speeds are unique to support the architecture.
3. Apply the settings to the serial port.

```
struct termios tty; //Create the struct
tcgetattr(fd, &ttyXX); //Get the current settings of the serial port
cfsetispeed(&ttyXX, B9600); //Set the read and write speed to 19200 BAUD
cfsetospeed(&ttyXX, B9600); //All speeds can be prefixed with B as a
settings.
// Where XX should be replaced with the type of port connected to communicate.
tty.c_iflag = 0;
tty.c_oflag = 0;
tty.c_cflag = 0;
tty.c_cflag |= CS8;
tty.c_cflag |= CLOCAL | CREAD;
tty.c_cc[VMIN] = 1;
tty.c_cc[VTIME] = 0;
// tty.c_cflag|=PARENB|PARODD;
// Now set the tty options (set immediately)
tcsetattr(fd, TCSANOW, &ttyXX);
tcsetattr(fd, TCSAFLUSH, &ttyXX);
// set the status flags
fcntl(fd, F_SETFL, O_NONBLOCK);
```

5.2.3 Reading and Writing data onto the Port

In Linux, the serial port is treated as a file, and the file operations(read/write) are used to send data to and from the port. These operations differ from standard file input/output operations in that the number of bytes to be read or written and

the number of bytes actually read or written are very important. It is a good idea to compare the number of bytes that were actually read/write to the number of bytes that were supposed to have been read/write to insure the correctness of the program and the accuracy of the data.
When reading or writing to the serial port, the programmer provides a pointer to a buffer containing the number of words to be written and the size of the buffer. The system then returns the actual number of words that have been read or written. The read and write functions return a boolean value, but this value does not relate to the success or failure of the operation. Only by checking the actual number of bytes read or written can the actual success of the operation be ascertained [15]. Code to read and write to a serial port can be found below:

```
/**********************************
Reading from the Serial Port
**********************************/
//fd is the file descriptor to the serial port
//command is a pointer the array we want to read data into
//bufSize is the amount of data that we want to read in
int serialRead = read(fd, command, bufSize);

/**********************************
Writing to the Serial Port
**********************************/
//write data to the serial port fd is the file descriptor of the serial
port
//buf is a pointer to the data that we want to write to the serial port
//bufSize is the amount of data that we want to write
int serialWrite = write(fd, command, bufSize);
```

5.2.4 Closing a Serial Port

It is not strictly necessary to close the port, because Linux reclaim all resources used by the application. It is however a good practice, to explicitly free all resources used so as to not rely on methods that can't be controlled. Some applications may still reside in memory even after the usage of the port, this make the lack of availability of the port for other application. For this reason, explicitly closing the port when it is no longer in use is a good habit to use [15].
Closing the serial port on Linux involves a single call to the close() system function, as the following code demonstrates.

```
 //close the serial port
if(close(fd) == -1) {
//Unable to open the port.  }
```

Chapter 6

Image Handling Protocol

According to the mission requirements, UART serial interface has been developed. Chapter 5 describes the configuration and modifications of the serial port settings. However configuring and opening the serial port doesn't satisfy our purpose, in order to access the various functionality of the payload one should be able to configure the CMOS image sensor at any given time and trigger it for the desired instant. For all these reasons, an image handling protocol is proposed and implemented, that can be followed by the user to gain access for the vision payload with the UART serial interface.
Such protocol can be defined by the control flow diagram described in 6.1. Commands for the vision payload functionality are defined by the identifiers that are set in accordance with the OBDH unit, identifiers that are used up by different sub systems are avoided to quash the duplicity.

Proposed Image Handling protocol shall consist the following functionality.

1. Commands to manual configure image acquisition parameters,
   e.g., resolution, windowing and sensor gains.
2. Trigger.
3. File transfer, listing, calculation of size etc.,
4. Calculate the temperatures of the PPU.
5. Indicate status of UART with LED.

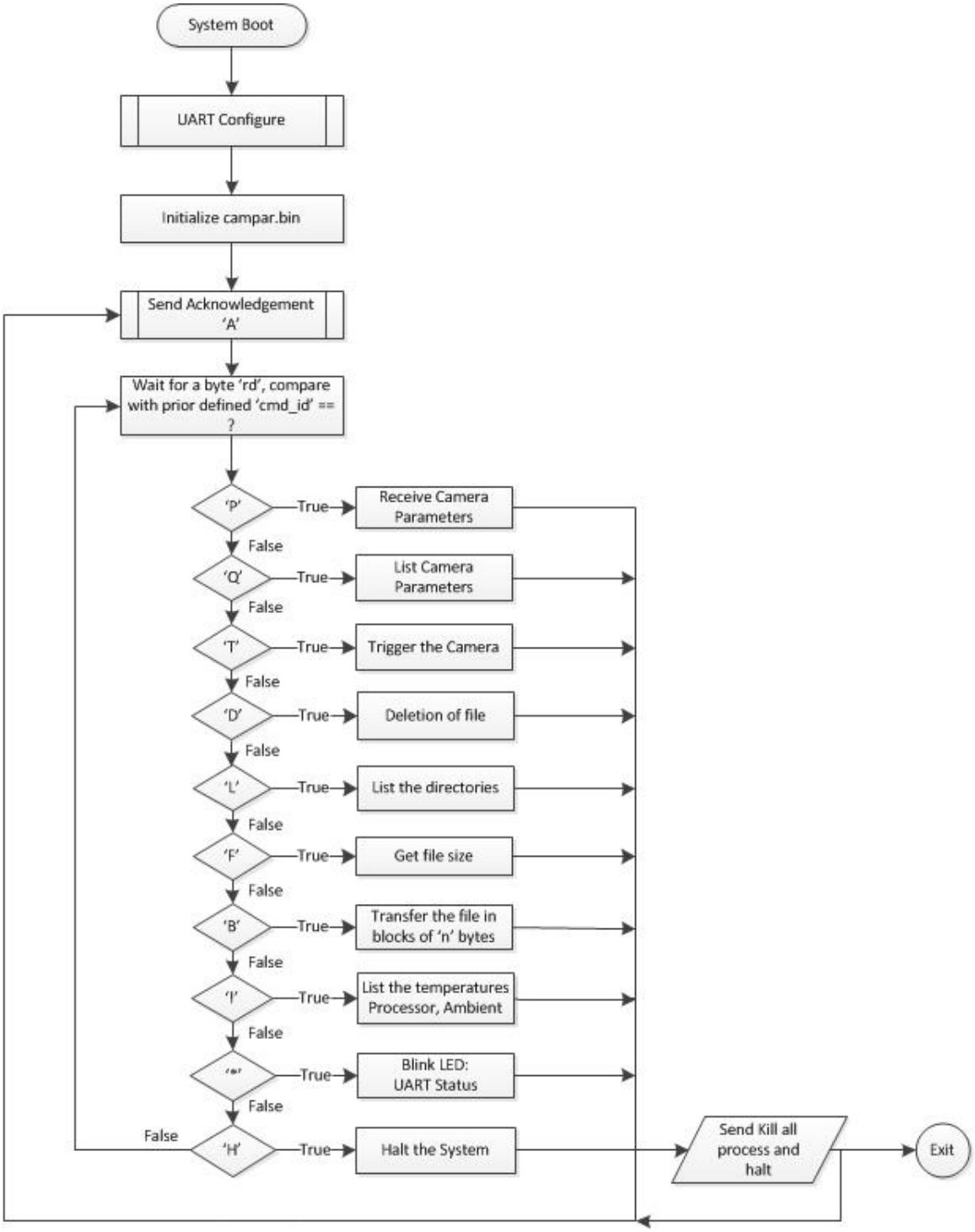

FIGURE 6.1: Image Handling Flow diagram

6.1 System Commands

system() executes a command specified in command by calling /bin/sh -c command, and returns after the successful execution of the command. Include the library *stdlib* to use system commands.

```
Command:
int system(const char * command);
```

If the Value of the command is NULL, system() returns non-zero if the shell is available, and zero if not. This type of execution is used in this thesis for multiple purposes, whenever standard shell commands are required to execute.

6.2 Camera Parameters

The performance of the CMOS image Sensor/Camera depends on the key parameters of the sensor like exposure frequency, exposure count, gain factor, ADC reference voltages etc., These parameters if configured with appropriate values can capture the images of good quality and can be of good use for remote sensing. For such reason, the Payload firmware has provided the provision to configure these key parameters from Ground Segment. In order to configure, first an identifier 'P (0x50)' is sent that signs the Payload to be configured followed by the parameters in HEX with respect to their type and later stored in 'campar.bin'.

6.3 Listing the configured Parameters

The configured parameters of the CMOS Sensor/Camera are stored in the *'campar.bin'* file, this binary file is parsed and read, to manually configure the sensor characteristics. Here after reception of this identifier 'Q (0x51)' at the payload end, PPU transmits the previous configured parameters for the requested device (e.g., OBDH Unit) in HEX format and is explained with and example in the table 6.1

6.4 Trigger the Camera

The Payload is triggered by executing the compiled program with the help of system commands as shown in the Figure 6.1 after the reception of the identifier 'T(0x54' followed by the slot ID to store after successful operation.

```
unsigned char sid;
int res = tty_read_chars(fd, sid, 1);
```

```
if (0 < res)
trigger_into(sid);
```

6.5 Deletion of the files

OBDH unit can delete the file directory through by command as in the table 6.1 after the transfer of the necessary requested file in order to free the memory at PPU. Multiple image file deletion can be also performed. This operation is performed by calling the routine dir_delete, this is interpreted by Payload via serial command 'D(0x44)' followed by the slot ID to remove from memory.

```
void dir_delete(int dir_num)
char command[200];
sprintf(command, "rm -r %s/%03i", root_dir, dir_num);
printf("trying to delete slot %i with[%s]", dir_num, command);
int res = system(command);
printf("result %i", res);
```

6.6 Listing of the files

When the user wants to know the information about the number of files stored and vacant slots available, he can call by the command 'L(0x4C)' via serial interface to list the available files. But our case here we call files as directories since, each directory is designed to store various file formats like raw, compressed and thumbnail formats of the same image files.

```
void list_directory(unsigned char dir_num[])
struct dirent *dp;
int dir_cntr = 0;
DIR *dir = opendir(root_dir);
while ((dp = readdir(dir)) != NULL)
if (strcmp(dp->d_name, ".") == 0 || strcmp(dp->d_name, "..") == 0)

else
int slot = atoi(dp->d_name);
dir_cntr++;
dir_num[dir_cntr] = slot;
```

```
printf("%s [%s] %i", root_dir, dp->d_name, slot);


closedir(dir);
dir_num[0] = dir_cntr;
```

TABLE 6.1: Reference Image Handling Protocol

Command	**Notation**	**HEX format output on Screen**
Configurable Parameters	P(0x50)	0x50 0x03 0x7A 0x03 0xFF 0x01 0xED 0x2F 0x28 0x03 0xC7 0x09 0xC7
Verify configuration	Q(0x51)	0x50 0x03 0x7A 0x03 0xFF 0x01 0xED 0x2F 0x28 0x03 0xC7 0x09 0xC7
Trigger for oneShot	T(0x54)	0x54 0x02 0x00 0x01 Followed by slotID to store
List the available images	L(0x4C)	0x01 0x4A 0x02 0x00 List all the directories
Deletion of image after transfer	D(0x44)	0x44 0x01 To delete the image folder
File Size	F(0x46)	0x46 0x02 0x03 0x00 0x00 0x7D 0xB6 32182 bytes Get file size of the particular image
Block Transfer	B(0x42)	0xFF 0xD8 0xFF 0xE0 0x00 0x10 0x4A 0x46 0x49... Transfer file in blocks of 8 bytes
System Halt	Halt(0x48 0x61 0x6C 0x74)	0x48 0x61 0x6c 0x74 AcknowledgmentACK
SBC Temperature	(0x21)	0x3C 0x30 0x00 Read chip temperature
LED Status	$*$(0x2a)	0x2a 0x00 (ON) 0x2a 0x01 (OFF) To test the interface working

6.7 Transfer of the file

The designated file that is to be to transferred is calculated for its size initially and then divided into blocks of desired size and transferred via serial interface to the user. Before, initiation of the file transfer, PPU calculates the size of the file that is requested by the OBDH unit and passes the information in the first byte of the file that is to be transferred. So, that the user (OBDH in our case) knows the estimated time of opening the port till the accomplishment if the task. However, each successful operation is acknowledged by an identifier `'A'`.

```
if (0 < strlen(global_fileTransfer.file_name))
fstream file(global_fileTransfer.file_name, ios::in | ios::binary |
ios::ate);
if (file.is_open())
global_fileTransfer.total = file.tellg();
printf("filesize is if (global_fileTransfer.total < 1000000)
file.seekg(0, ios::beg);
global_fileTransfer.content = new char[global_fileTransfer.total +
block_size];
file.read(global_fileTransfer.content, global_fileTransfer.total);
printf("acquired content");
else
printf("file is too large to transfer!");

file.close();
else
printf("cannot open file");
```

6.8 List the temperatures

Absolute & ambient temperatures of the AMD chip can be directly accessed, calling built in methods. With this temperatures somehow, we can estimate the operating temperature of the payload.

```
struct sbc_temperatures mySbcTemp = getTemperatures();
write(fd, mySbcTemp, sizeof mySbcTemp);
```

6.9 Halt the System

The Payload can be halted using the system commands to save the power,whenever it is not in use and an acknowledgement ‘vj’is sent to the user.

```
unsigned char msg[3];
int read_num = tty_read_chars(fd, msg, 3);
if (read_num == 3)
if (msg[0] == 'a'  msg[1] == 'l'  msg[2] == 't')
unsigned char echo[2];
echo[0]='v';
echo[1]='j';
write(fd,echo,1);
system("halt");
write(fd,echo+1,1);
exit(0);
```

Chapter 7

Conclusion & Future Work

7.1 Summary of the Thesis

Vision payload for the Nano Satellite VELOX-I has been developed in compliance to the standards of the 3U CubeSat. Study and implementation of CCSDS recommended image compression algorithm has been presented and implemented in MATLAB. In order to estimate the best suitable sensor parameters for imaging, GUI in Java has been developed and tested. In house developed radiation hardened sensor has been calibrated for best performance with the developed firmware. Fixed Pattern Noise of the sensor is eliminated before storing the final image. A thorough literature on UART serial interface development has been presented and implemented in the Payload firmware. Lastly, image handling protocol has been proposed and documented for the users to access the Payload. Necessary instructions and setup procedure has been given in the Appendix for user reference. Combining all, the objectives of the thesis have been successfully accomplished. The firmware developed serves as the core for the Payload of its kind and is the base platform for further application development.

7.2 Future Work

The Payload developed for the mission VELOX-I comprises of three modules namely, sensor Board, acquisition board and the processing unit. Efficient utilization of mass, size and power of CubeSat mission impose constraints over the current developed payload. For future similar missions, this architecture consisting of three boards can be replaced by the single System On Chip and processor board. Furthermore applications of the Payload can be extrapolated to Star Sensor, debris monitoring over current mono Earth observation functionality. These

applications can be easily build as an extra function without the major changes in the core firmware. Analysis and calculations of the optics and sensor at extreme environments is to be performed.

Appendix A

Linux Installation Procedure

Prepared by : Vineel Kadarla & Jan Hakenberg
Date: 2012-Aug-08
Purpose: Project Reference Manual
Target Board : Cool SpaceRunner - LX800 PC/104-Plus SBC

1. Create a bootable USB-drive with debian squeeze 2.6.32-5.
2. Power on the SBC and press F1 to enter into BIOS mode.
   Change the Boot Preference order with USB/Flash to the first position.
   Press X, to save and exit.
3. Reboot the SBC.
4. Choose “Install” in the welcome screen.
5. Choose Language “English”.
6. Choose Location “Singapore”.
7. Choose Keyboard Layout “American English”
8. During installation, ignore the notification *e100/d102e_ucode.bin*
   is missing by selecting “NO”.
9. Ignore notification that network configuration has failed.
10. Do not configure at this time.
11. Enter the Host name (e.g., veloxn).
12. Enter the name of the user (e.g., leonie).
13. Enter the username (e.g., leonie).
14. Enter the user password (e.g., root).
15. Choose guided partitioning (Primary option).
    Here it shows your USB drive details and target SSD.
    Choose target SSD (scsi1 sda ATA 2GB).

16. All in one partition
17. Finish partitioning
18. Select “yes” to write to disc
19. Install ssh server (press space to select)
20. Install GRUB boot loader
21. Finish installation by removing usb drive and rebooting

Appendix B

Missing Packages

B.1 Intel Network Packages

During installation of Linux (Debian), some of the binary firmware for the various drivers in the Linux kernel mayn't be properly installed. For, our case network packages were erratic while installation. In order to reassure the drivers working properly one need to download the "Firmware-linux-nonfree" for the respective kernel and store them on a removable media and mount the device whenever asked during installation or manually port them after the completion of the installation process.

1. Store the downloaded executable in removable media,
   `dpkg -i firmware-linux-nonfree_0.28+squeeze1_all.deb`
2. As root, create folder: `$sudo mkdir ~/mnt/myusb.`
3. Mount the removable media (eg., Flash drive): `$mount /dev/sdb1 /mnt/mysub.`
4. Copy the above file to the desired location.
5. Depackage it to manually port the drivers,
   `$dpkg -i firmware-linux-nonfree_0.28+squeeze1_all.deb`

B.2 Enable network interfaces

To ensure the network bring up , one should edit the file 'interfaces" located at `/etc/network`

1. `command :`
   `$nano /etc/network/interfaces or`
   `$vi /etc/network/interfaces`
   `file content:`
   `auto lo`
   `iface lo inet loopback`
   `#DHCP Configuration`
   `allow-hotplug eth0`
   `iface eth0 inet dhcp`

2. After installation, don't forget to bring up the interface which is scripted recently,
   `command:`
   `$ifup eth0`

3. Now, check the network configuration with the commands `$ifconfig`. Following the above procedure, one should be able to view ip address for the respective network. Otherwise something went wrong, go to step 1 and continue.

B.3 Locating the package repository

Check if proper repositories are listed in `/etc/apt/sources.list`, otherwise edit the list with

```
command:
$sudo nano /etc/apt/sources.list
// add these lines to it and save it
deb http://security.debian.org/ squeeze/updates main contrib non-free
deb-src http://security.debian.org/ squeeze/updates main contrib non-free
deb http://ftp.debian.org/debian/ squeeze main contrib non-free
deb-src http://ftp.debian.org/debian/ squeeze main contrib non-free
deb http://ftp.debian.org/debian/ squeeze-updates main contrib non-free
deb-src http://ftp.debian.org/debian/ squeeze-updates main contrib non-free
```

Apart from the above repository locations, try to find the address of the local nearest repository for the respective kernel installed and add them to the above file accordingly.

B.4 To reload the rules in Ubuntu/Debian without restart

`command:`
`$sudo /etc/init.d/udev restart`
Don't forget to key in the appropriate root password.

B.5 Enabling default root logging

For applications like ours, in which the system should be in root mode to execute the necessary privileges of the functionality of the payload (application framework) and configure the firmware from third party device with an interface without the intervention of keying in the password every time when kernel layer is accessed.

1. Look for the shell script in /etc/inittab and edit it. `command:`
   `$nano /etc/inittab`
2. Identify the following line
   `1:2345:respawn:/sbin/getty 38400 tty1` and comment out as
   `#1:2345:respawn:/sbin/getty 38400 tty1`
3. Add the following line instead of the earlier
   `1:2345:respawn:/bin/login -f root tty1 /dev/tty1 >/dev/tty1 2>&1`
4. Save and exit the file.
5. Reboot the system to enable the root logging after boot.

Appendix C

Specification Documents

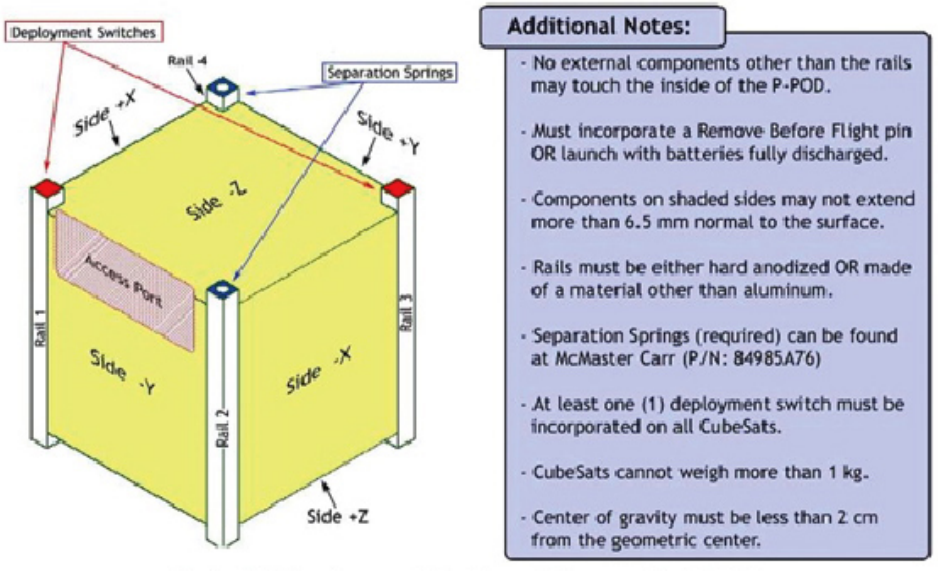

Figure C.1: 1U CubeSat Specifications

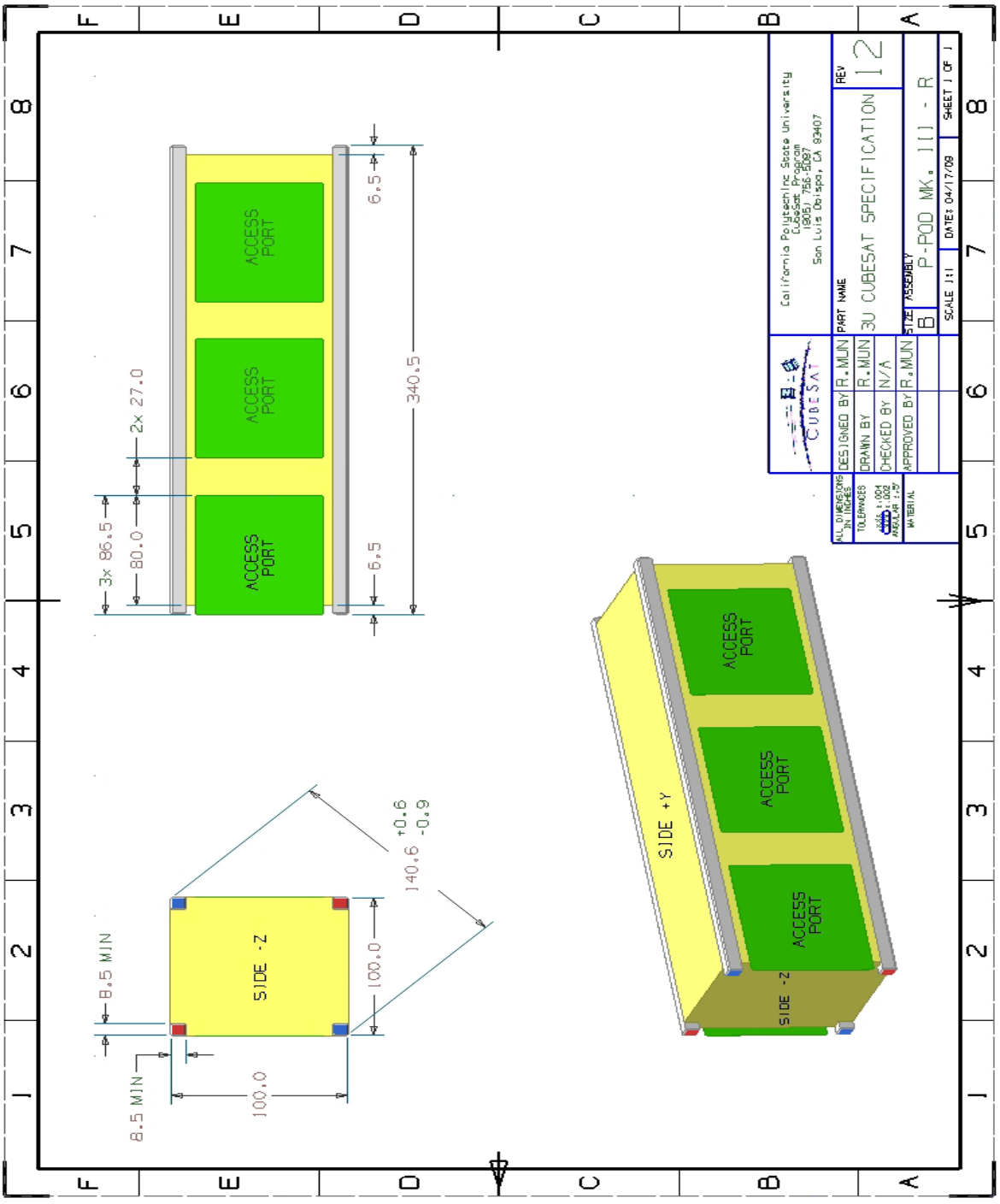

FIGURE C.2: 3U CubeSat Specifications

Bibliography

[1] Prof.Sumana Gupta. Digital image processing. online-NPTEL.

[2] Sharadha. Image compression algorithms onboard of small satellites. Master's thesis, SCE, Nanyang Technological Univeristy, 2011.

[3] Rod Bird. Accessing serial port. WikiSpaces. URL ibpe.wikispaces.com/AccessingSerialPort. Retrieved on 12th August,2012.

[4] Image data compression (recommended standard ccsds 122.0-b-1). URL http://public.ccsds.org/publications/documents/IEEE_2005BigSky_PaperF1165_final.pdf.

[5] Tamer T.Elazhary Ayman Mahmoud and Amal Zaki. Remote sensing cubesat. *International society for optics and photonics*, 7826:8, October 2010.

[6] Riki Munakata. Cubesat design specification. online, January 2009. URL http://www.cubesat.org/images/developers/cds_rev12.pdf. Retrieved on 4th July, 2012.

[7] Richard Bui. VELOX - I first singapore nanosatellite. SaRC Booklet, August 2010.

[8] *Opal Kelly User Manual*. Opal Kelly.

[9] Silicon Imaging Inc. CMOS imaging fundamentals. online. URL http://www.siliconimaging.com/cmos_fundamentals.htm. Retrieved on 10th Aug, 2012.

[10] *Space Coolrunner Single Board Computer*. Lippert Embedded GmBH, 2010. URL http://www.adlinktech.com/PD/web/PD_detail.php?cKind=&pid=1148&seq=&id=&sid=&source=.

[11] Rafael C.Gonzalez & Richard E.Woods. *Digital Image Processing*. Prentice Hall, third edition, August 2007.

[12] Bo Zhao Shoushun Chen Xinyuan Qian, Hang Yu and Low Kay Soon. Design of a radiation tolerant cmos image sensor. Integrated Circuits (ISIC), 2011.

[13] David Krejci Daniel Selva. A survey and assessment of the capabilities of cubesats for earth observation. *Acta Astronautica*, 74(50):19, February 2012.

[14] *CYPLL221150 Manual*. Cypress Semiconductors.

[15] Michael R. Sweet. *Serial Programming Guide for POSIX Operating Systems*. Number 6th Revision in GNU Free Documentation License. 5th edition, 1994-2005. URL http://www.easysw.com/~mike/serial/.